

# Plasma Startup via Local Helicity Injection and Stability Studies at Near-Unity Aspect Ratio in the Pegasus Experiment

R.J. Fonck, J.L. Barr, M.W. Bongard, M.G. Burke,  
E.T. Hinson, A.J. Redd, N. Schoenberg,  
D.J. Schlossberg, K.E. Thome

*The Joint Meeting of 5th IAEA Technical Meeting on Spherical Tori*

*16th International Workshop on Spherical Torus (ISTW2011)*

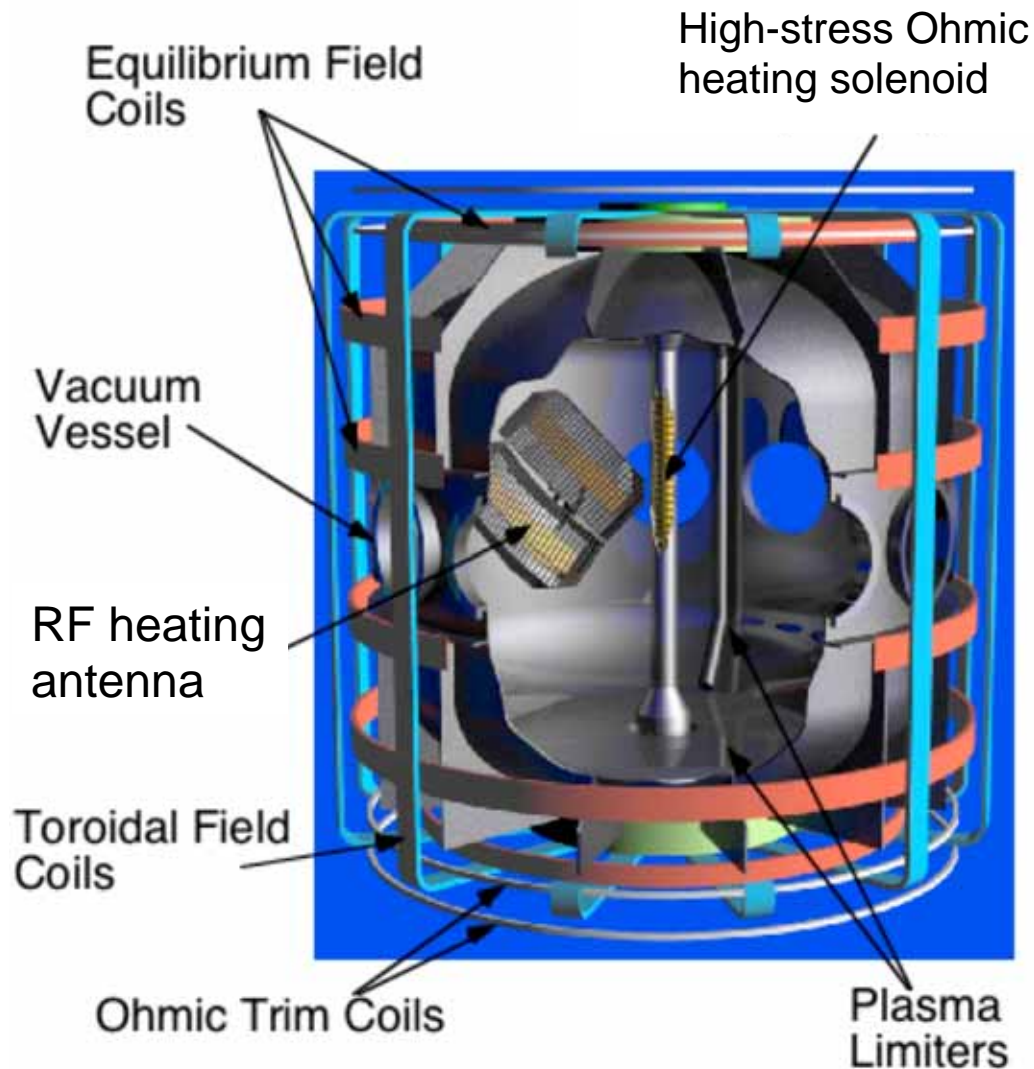
*2011 US-Japan Workshop on ST Plasma*

*National Institute for Fusion Science, Toki, Japan September 27-30, 2011*





# PEGASUS is a Compact Ultralow-A ST



## Experimental Parameters

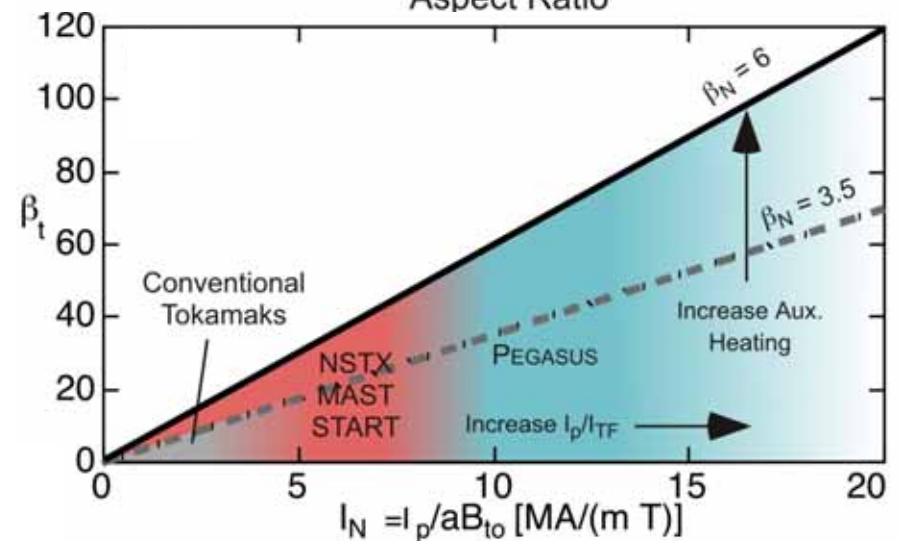
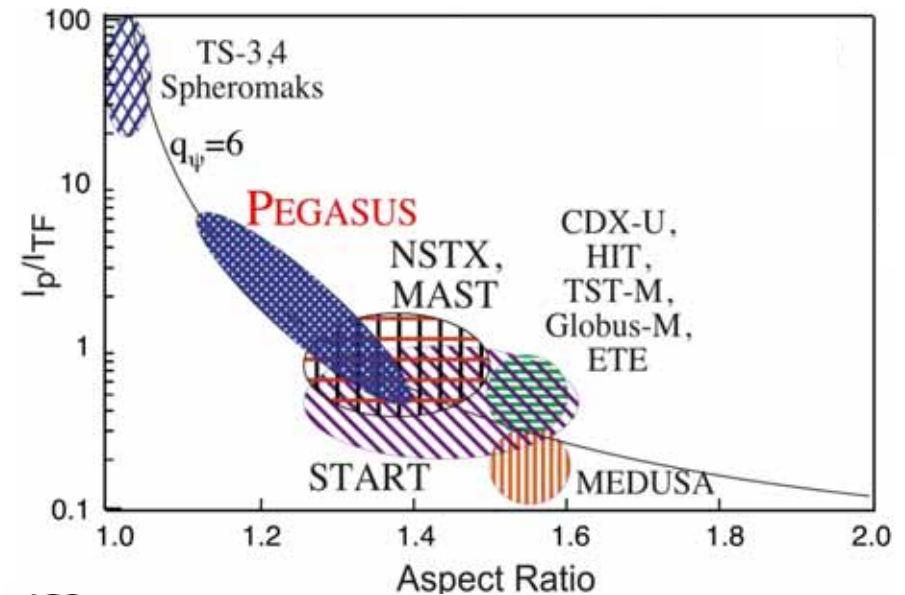
<u>Parameter</u>	<u>To Date</u>
A	1.15 – 1.3
R(m)	0.2 – 0.45
$I_p$ (MA)	$\leq .22$
$I_N$ (MA/m-T)	6 – 12
$l_i$	0.2 – 0.5
$\kappa$	1.4 – 3.0
$\tau_{\text{shot}}$ (s)	$\leq 0.025$
$\beta_T$ (%)	$\leq 25$
$P_{\text{HHFW}}$ (MW)	0.2





# PEGASUS Mission: Physics of Low $A \rightarrow 1$

- University-scale, Low-A ST
  - $R_0 \leq 0.45$  m,  $a \sim 0.40$  m
- Physics of High  $I_p/I_{TF}$ 
  - Expand operating space of the ST
  - Study high  $\beta_T$  plasmas as  $A \rightarrow 1$
- Non-solenoidal startup
  - Point-source helicity injection
  - Helicity injection discharges couple to other current drive methods
- Peeling-mode studies
  - Experimental tests of peeling-ballooning theory (ELM, ITER)

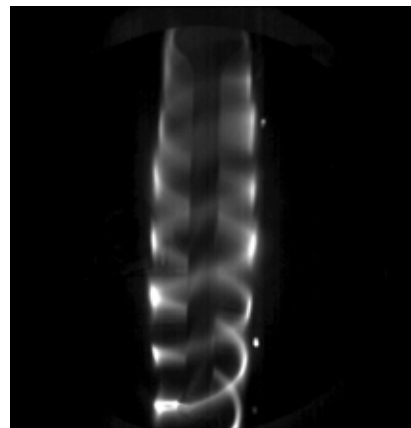






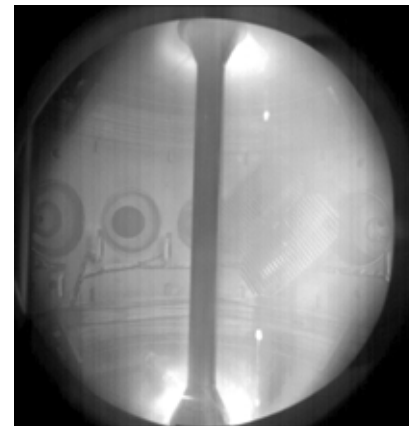
## Local Plasma Current Sources + Helical Vacuum Field Give Simple DC Helicity Injection Scheme

- Current is injected into the existing helical magnetic field
- High  $I_{inj}$  & modest  $B \Rightarrow$  filaments merge into current sheet
- High  $I_{inj}$  & low  $B \Rightarrow$  current-driven  $B_\theta$  overwhelms vacuum  $B_z$ 
  - Relaxation via MHD activity to tokamak-like Taylor state w/ high toroidal current multiplication



Current filaments

Reduced  $B_z$   
→



Relaxed tokamak

- Technical attractiveness: can remove sources and anode after startup



# DC Helicity Injection Startup on PEGASUS Utilizes Localized Washer-Gun Current Sources

- Plasma gun(s) biased relative to anode:

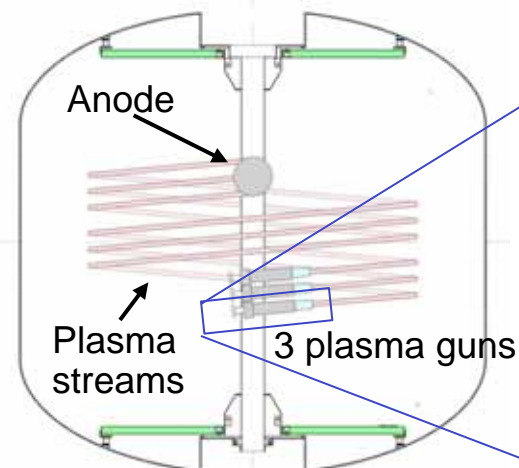
- Helicity injection rate:

$$\dot{K}_{inj} = 2V_{inj}B_N A_{inj}$$

$V_{inj}$  - injector voltage

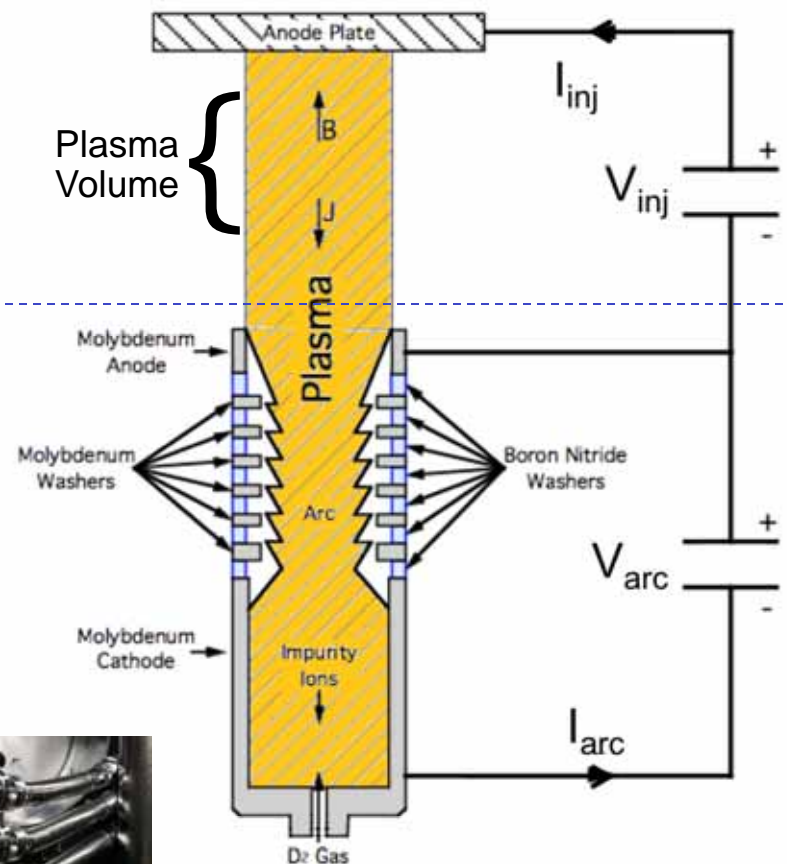
$B_N$  - normal B field at gun aperture

$A_{inj}$  - injector area



Midplane Injection

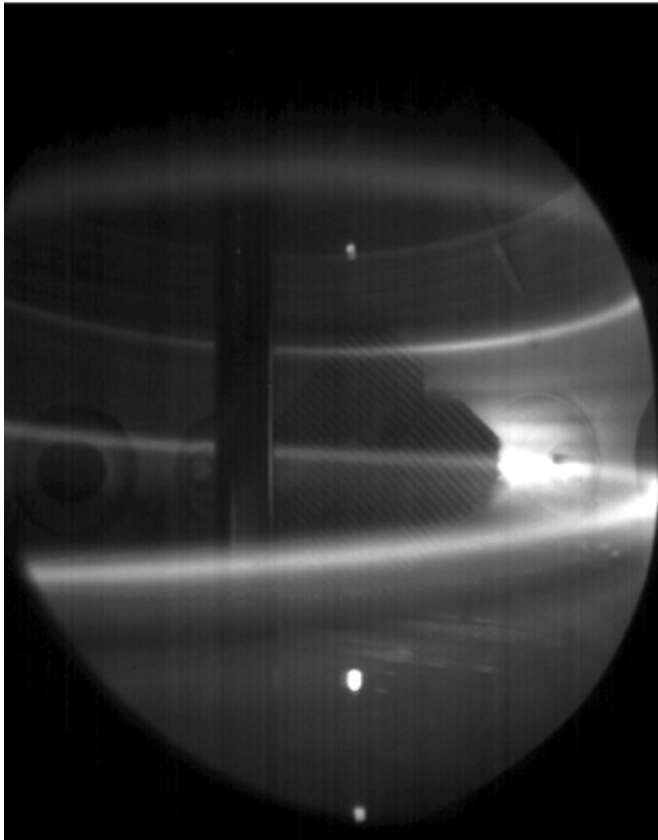
Simplified illustration of a plasma gun for helicity injection  
(not to scale)



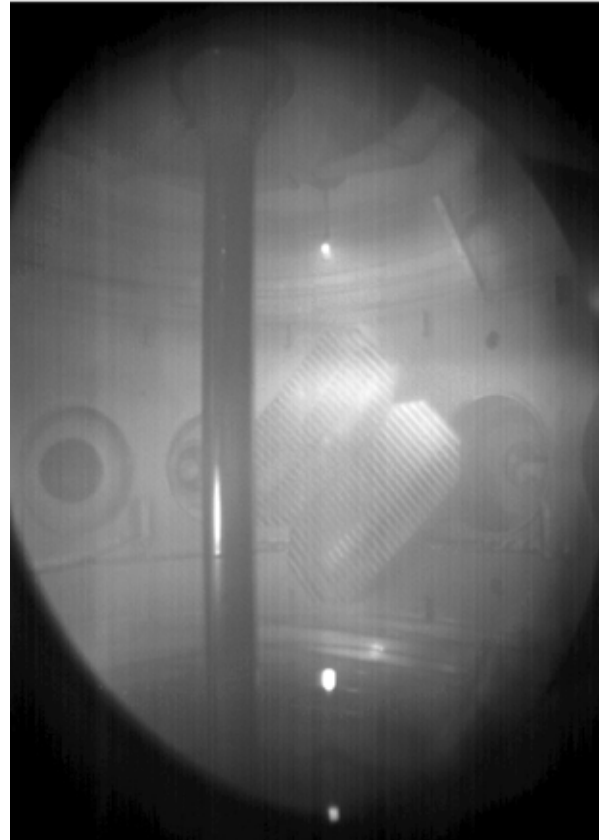


# Evolution of midplane-gun-driven plasma

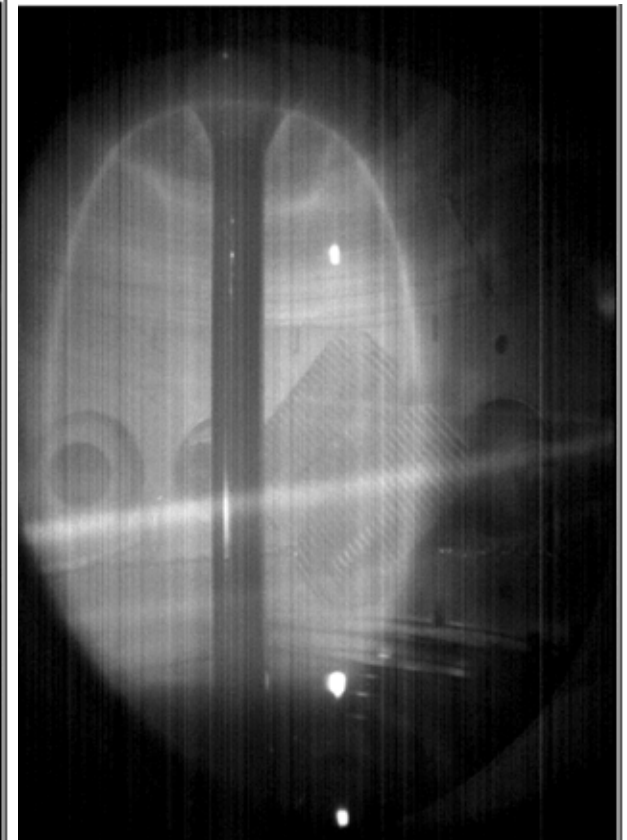
PEGASUS shot #40458: two midplane guns, mild outer-PF ramp



$t=21.1$  ms,  $I_p=2-3$  kA  
Filaments only



$t=28.8$  ms,  $I_p=42$  kA  
Driven diffuse plasma



$t=30.6$  ms,  $I_p=37$  kA  
Guns off, Decaying



# Taylor Relaxation Criteria Sets the Maximum $I_p$ for a Given Magnetic Geometry

Helicity balance in a tokamak geometry:

$$\frac{dK}{dt} = -2 \int_V \eta \mathbf{J} \cdot \mathbf{B} d^3x - 2 \frac{\partial \Psi}{\partial t} \Psi - 2 \int_A \Phi \mathbf{B} \cdot d\mathbf{s} \quad \longrightarrow \quad I_p \leq \frac{A_p}{2\pi R_0 \langle \eta \rangle} (V_{ind} + V_{eff})$$

- Helicity injection can be expressed as an effective loop voltage
- $I_p$  limit depends on the scaling of plasma confinement via the  $\eta$  term

$$V_{eff} \approx \frac{A_{inj} B_{\phi, inj}}{\Psi_T} V_{bias}$$

Taylor relaxation of a force-free equilibrium:

$$\begin{aligned} \nabla \times \mathbf{B} = \mu_0 \mathbf{J} = \lambda \mathbf{B} \\ \lambda_p \leq \lambda_{edge} \end{aligned} \quad \longrightarrow \quad \frac{\mu_0 I_p}{\Psi_T} \leq \frac{\mu_0 I_{inj}}{2\pi R_{inj} w B_{\theta, inj}} \quad \longrightarrow \quad I_p \leq \left[ \frac{C_p}{2\pi R_{inj} \mu_0} \frac{\Psi_T I_{inj}}{w} \right]^{1/2}$$

Assumptions:

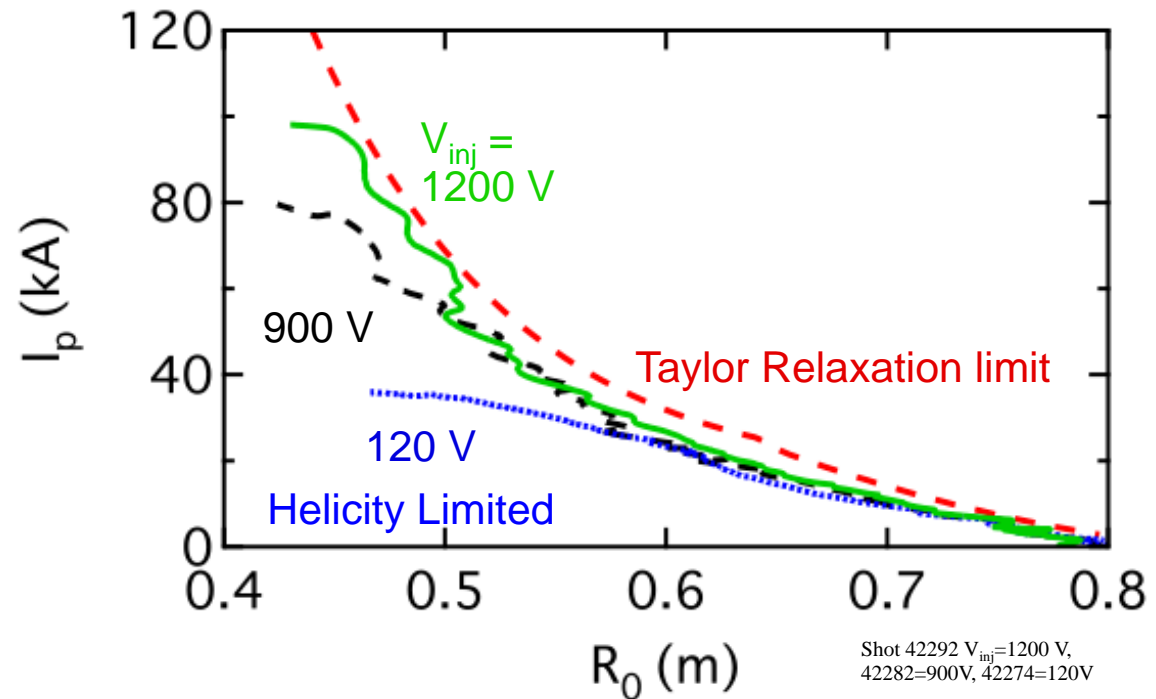
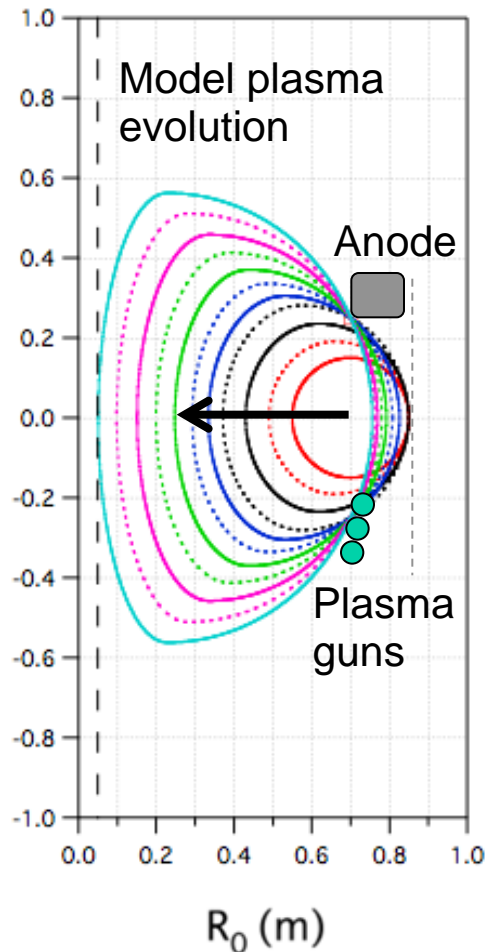
- Driven edge current mixes uniformly in SOL
- Edge fields average to tokamak-like structure

$A_p$	Plasma area
$C_p$	Plasma circumference
$\Psi_T$	Plasma toroidal flux
$w$	Edge current channel width





# Achieving the Maximum $I_p$ at the Taylor Limit Requires Sufficient Helicity Injection Input Rate



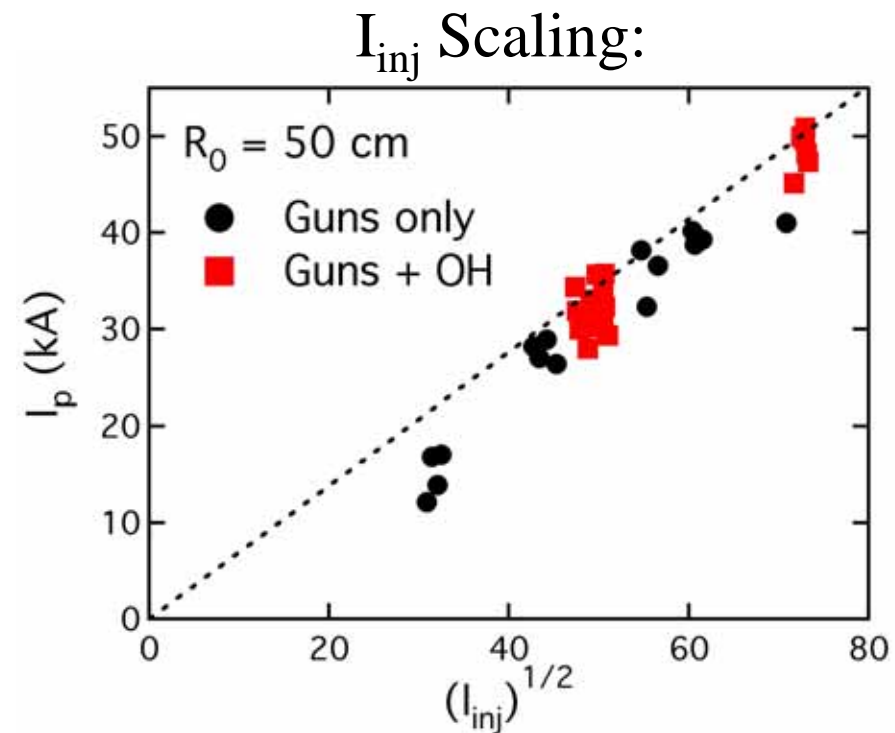
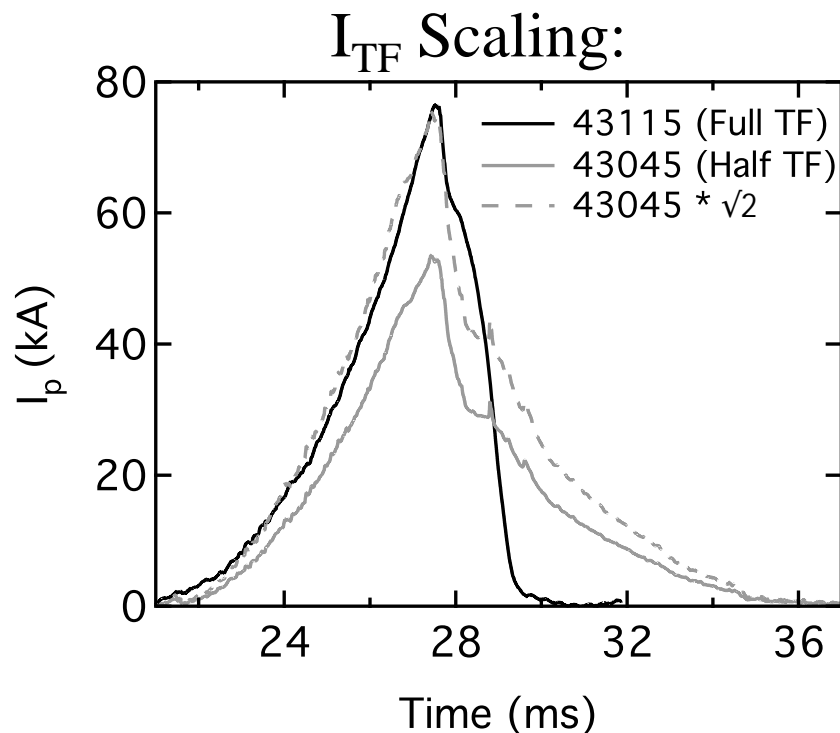
- Helicity input rate, and effective net volt-seconds, increases as  $V_{inj}$  increases
- Sufficient net V-sec needed to reach Taylor relaxation limit





# Experiments Confirm Relaxation Limit Scalings with $I_{TF}$ and $I_{inj}$

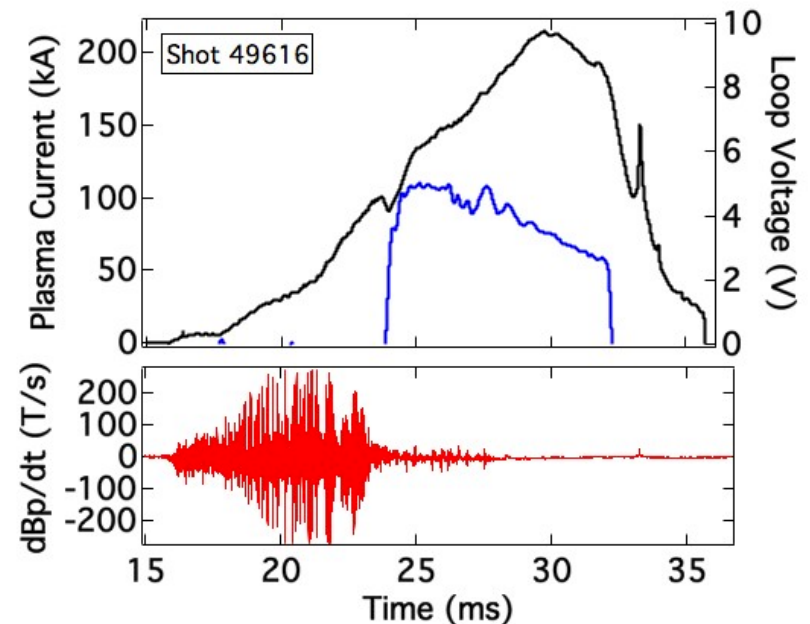
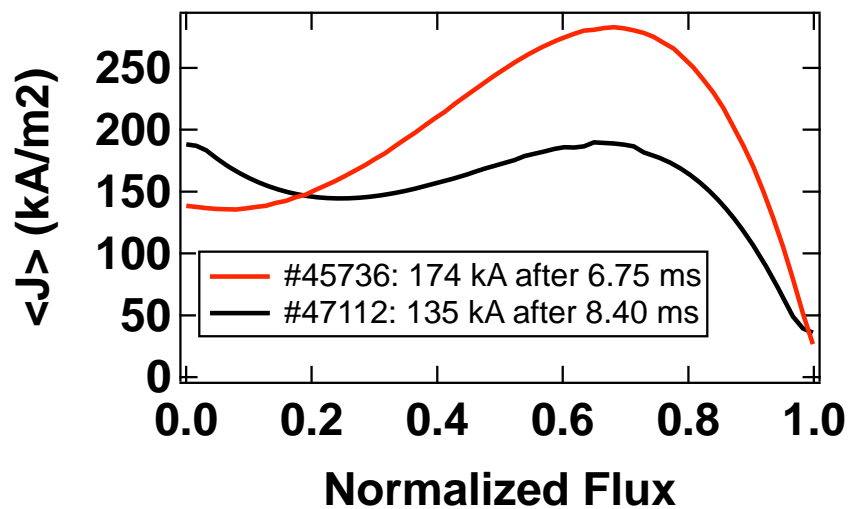
- The relaxation limit  $I_p$  scales with: 
$$I_p \propto \left[ \frac{I_{TF} I_{inj}}{W} \right]^{1/2}$$
- Experimental plasma current limits follow these scalings:





# Slowly-evolving Gun-driven Plasmas Hand Off Most Efficiently to Ohmic Drive

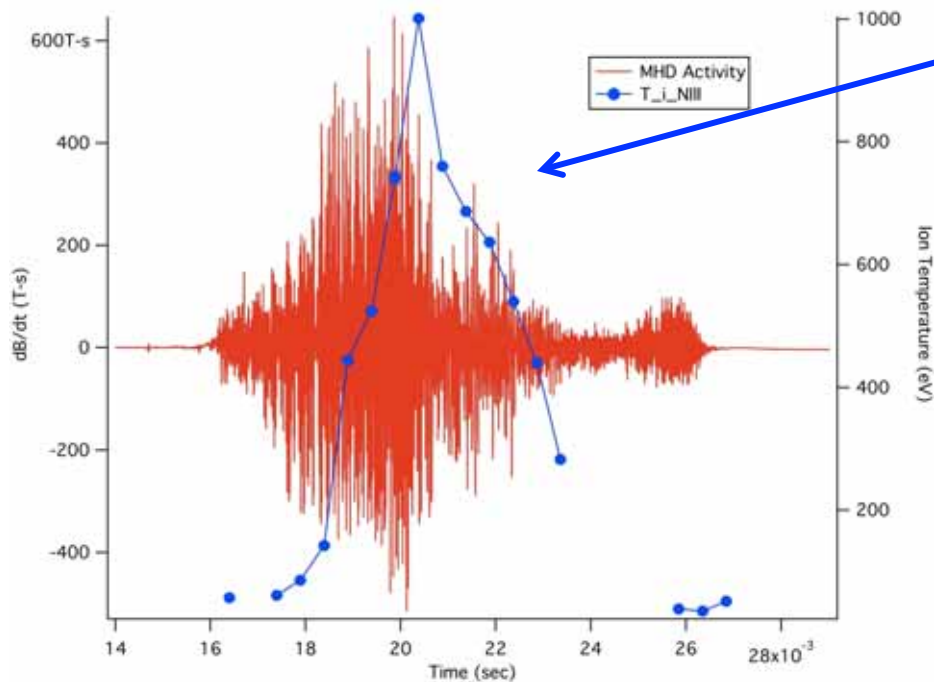
- Poloidal flux generated by helicity injection is equivalent to that generated by Ohmic Drive
  - $I_{\text{total}} = I_{\text{HI}} + I_{\text{OH}}$
- Excessive skin current => poor coupling to OH drive
- Slowly evolving: ~ flat  $j(r)$  (black)
  - Smooth handoff to Ohmic inductive drive ( $j(R)$  profiles from external-only equilibrium reconstructions;  $l_i < 0.3$ )
- Rapidly evolving: ~ hollow, strong skin  $j(r)$  (red)
  - Does not hand off efficiently to Ohmic drive





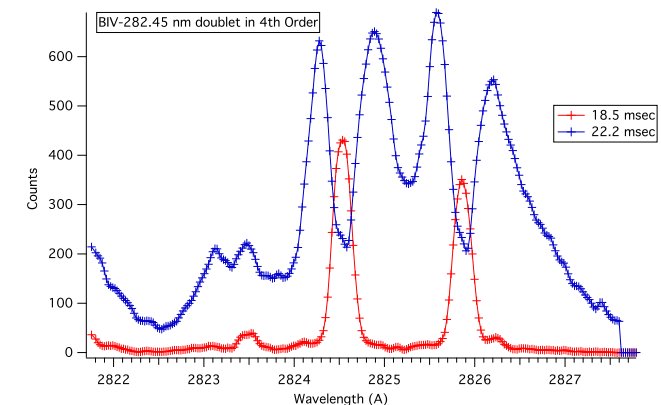
# Initial Spectroscopy Measurements Suggest Energetic Ions

- Spectroscopic  $T_i$  suggest high ion energies during reconnection period



Doppler  $T_i$  from radial view

Complex multi-line structures from tangential view



- However, situation is much more complex if viewed toroidally
  - Need improved time-resolution and spatial scans



# Several Issues to Address for a Predictive Model

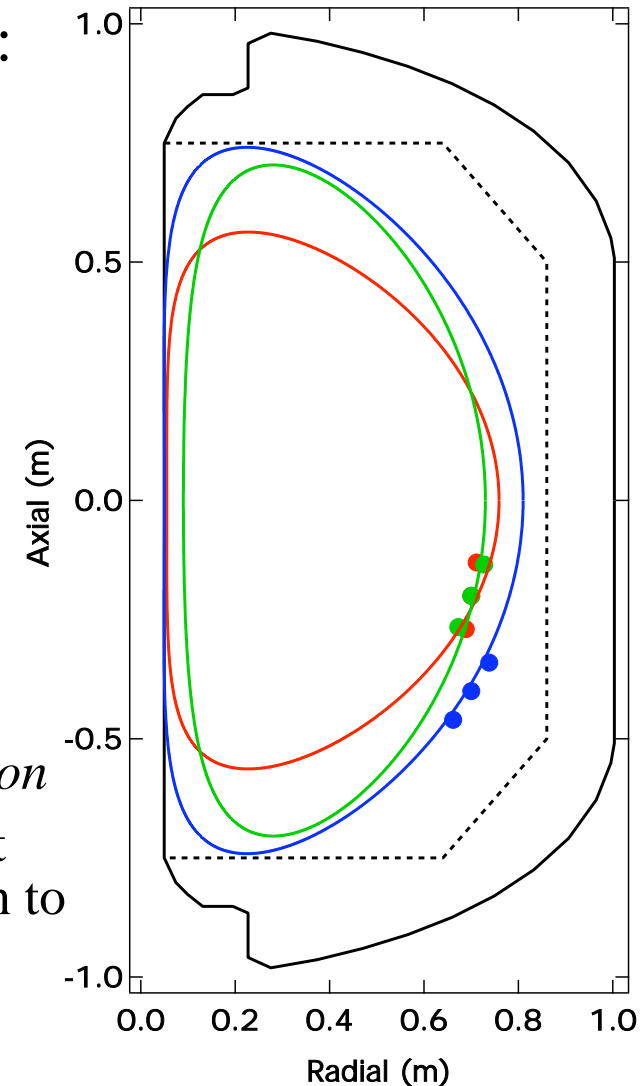
- Extension to higher current, longer pulse
  - Verify limit scalings
  - Discharge evolution for long growth phase
  - Test confinement properties, especially  $T_e(r,t)$ 
    - Helicity dissipation scaling model
- Optimal gun-electrode configuration
- Increased helicity injection rate
  - Test regime where helicity drive dominates PF induction for growth
  - Active guns vs. passive electrode approach for long-pulse growth
- Injected current source impedance model
  - What sets helicity injection rate?
- Edge  $j(r)$  measurements and  $\lambda(\psi,t)$ 
  - Physics of ultimate relaxation limits
  - Current transport: MHD behavior
- Impurity assessment and control





# Gun-Electrode Geometry: PF Induction, Plasma Size, and Null Formation

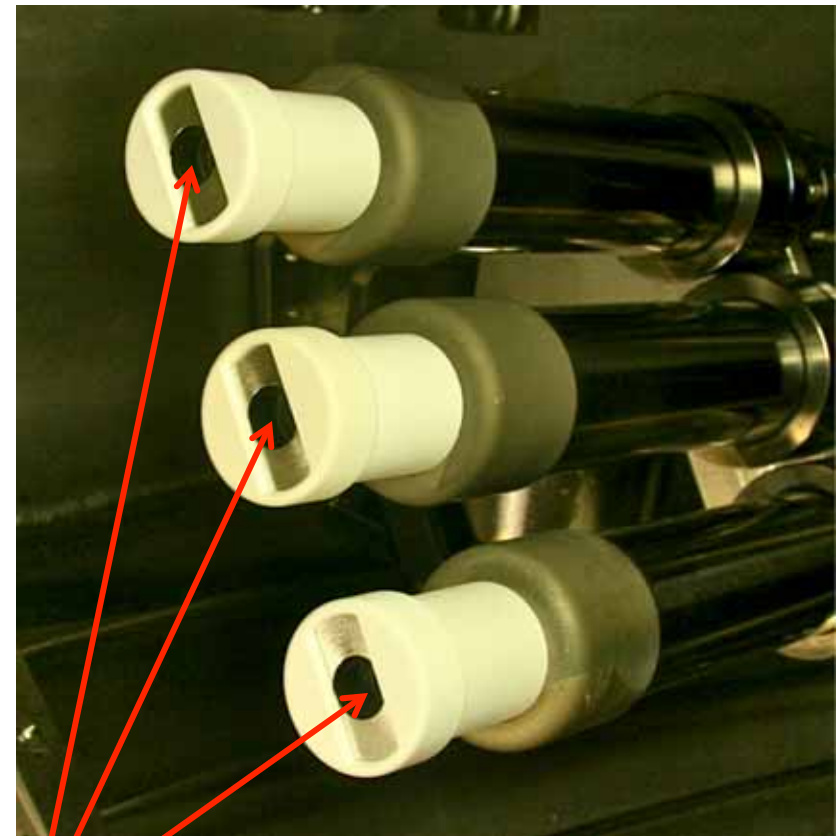
- Original: array was nearly vertical (red):
  - $J_{\text{edge}}$  width  $w$  scaled with # of guns
  - Maximum  $I_p = 0.11$  MA.
- Aligned gun array tilt (green):
  - Maximum  $I_p = 0.17$  MA.
  - 3-fold reduction in  $w$ ., consistent with changing the projected width at midplane.
- Maximize plasma size: array moved further away from midplane (blue):
  - Maximum  $I_p \sim 0.13$  MA
  - Larger startup plasma = *reduced PF induction*
  - *Poorer poloidal field null* formed by current streams = more difficult to induce relaxation to tokamak state
- Tight gun-anode geometry preferred





# Active Gun / Passive Electrode Assembly Points to Simpler, Higher $I_p$ Operation

- Potential for much higher  $I_{inj}$  without need for either more plasma guns or larger guns.
- Helicity injection physics is agnostic to the exact source of the edge charge carriers.
- Passive electrodes allow arbitrary shaping:
  - Can optimize both helicity input (large cross-sectional area) *and* the Taylor limit on  $I_p$  (narrow in radial direction)

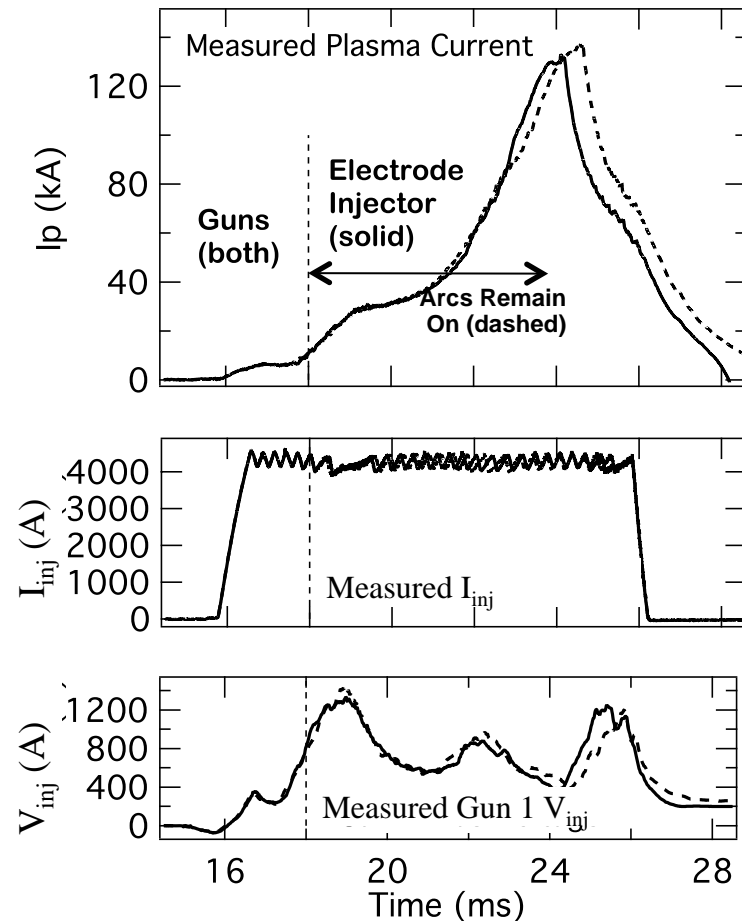


Plasma Guns with Integrated Slotted Electrodes



# Initial Tests of Gun/Electrode Helicity Injection System Are Promising

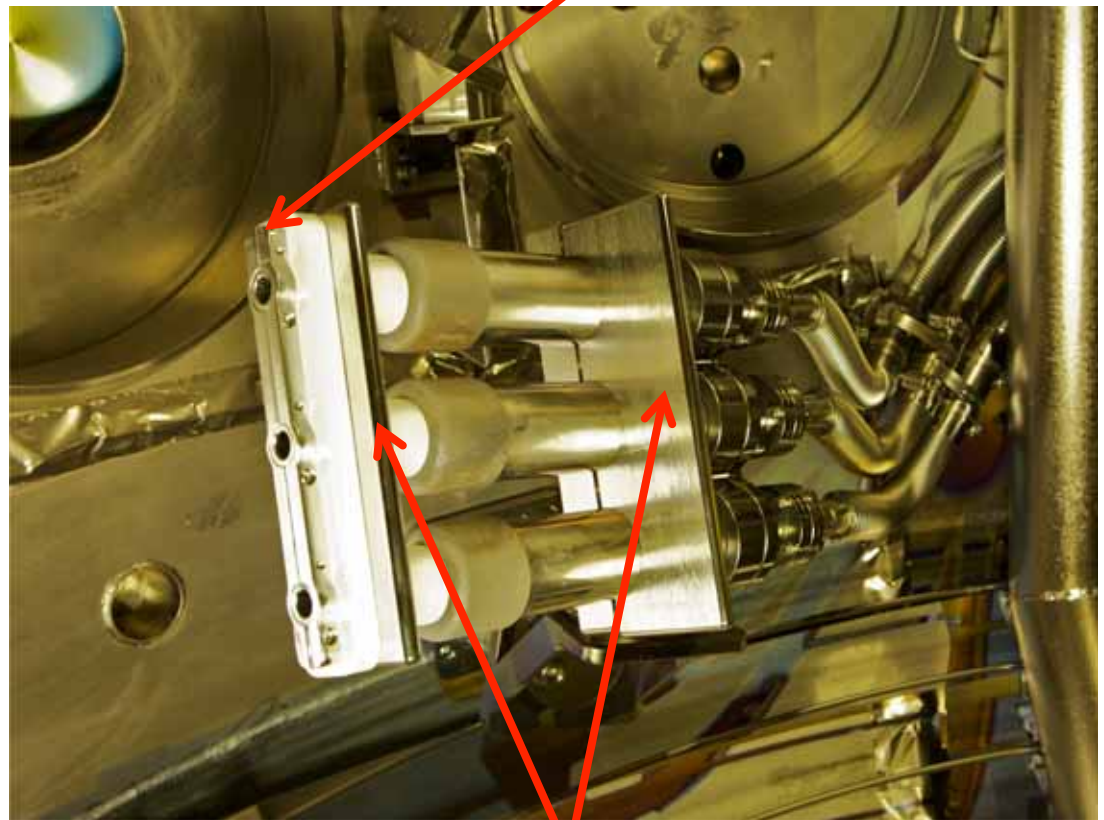
- Operations use two steps:
  - 1. Form initial tokamak-like state with minimal active arc gun
  - 2. Grow to much larger  $I_p$  with passive electrodes fed by electrode charge carriers induced and moderated by tokamak edge plasma.
- First tests are promising
  - Arc current off after relaxation and formation of tokamak-like state
  - $I_p$  rise is virtually the *same*, whether arc discharge or passive electrode provide the charge carriers





# Integrated Arc Gun – Passive Electrode Experiments Begun

- New gun-electrode assembly has extended electrode coupled to arc gun exit cathodes
  - Offers 5-times increase in helicity injection rate
- Integrated scraper limiters to protect assembly and control local edge density
  - Gas-puff control of  $V_{\text{bias}} \sim V_{\text{loop, effective}}$



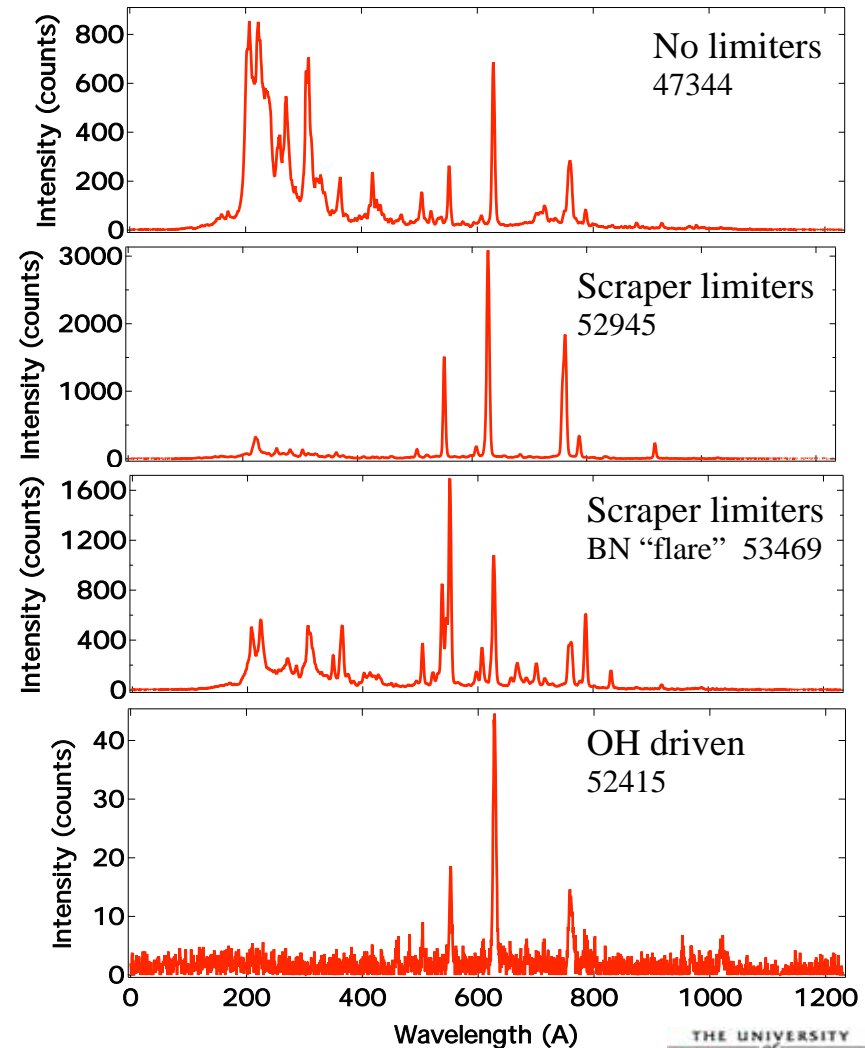
*Local limiters*





# Local Limiters Reduce N to Negligible Levels in Well-behaved Injection Cases

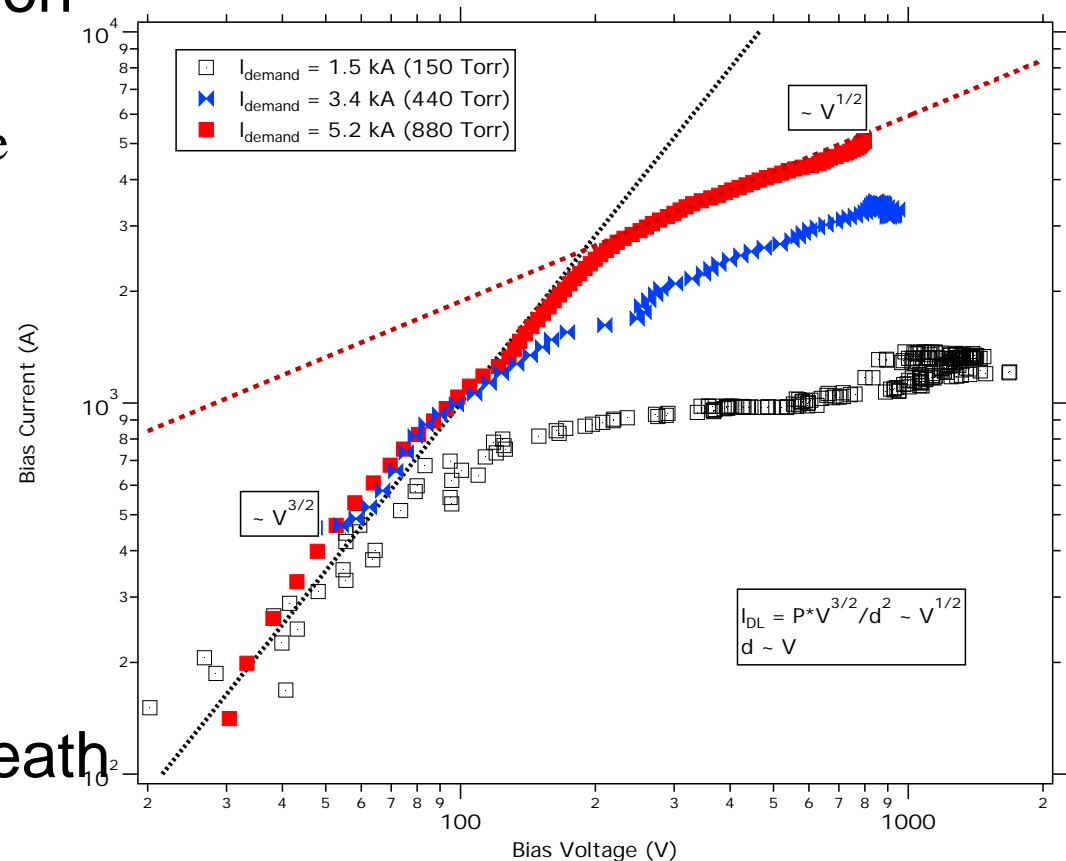
- N dominant impurity with unprotected gun assembly
  - 1<sup>st</sup> estimates of impurity content via bolometer measures
    - $Z_{\text{eff}} \sim 2.2. \pm 0.8$  during injection;  $\leq 1.4$  after injection
    - Mainly N;  $n_e \sim 5 \times 10^{18} \text{ m}^{-3}$  to  $2 \times 10^{19} \text{ m}^{-3}$
- Local scraper limiters much reduce N, O remains
- Bursts of N still evident with flare at BN surface
- Ohmic-only reference plasma very clean
  - $Z_{\text{eff}} \leq 1.2$





# Source Impedance Appears to be Governed by Sheath Physics

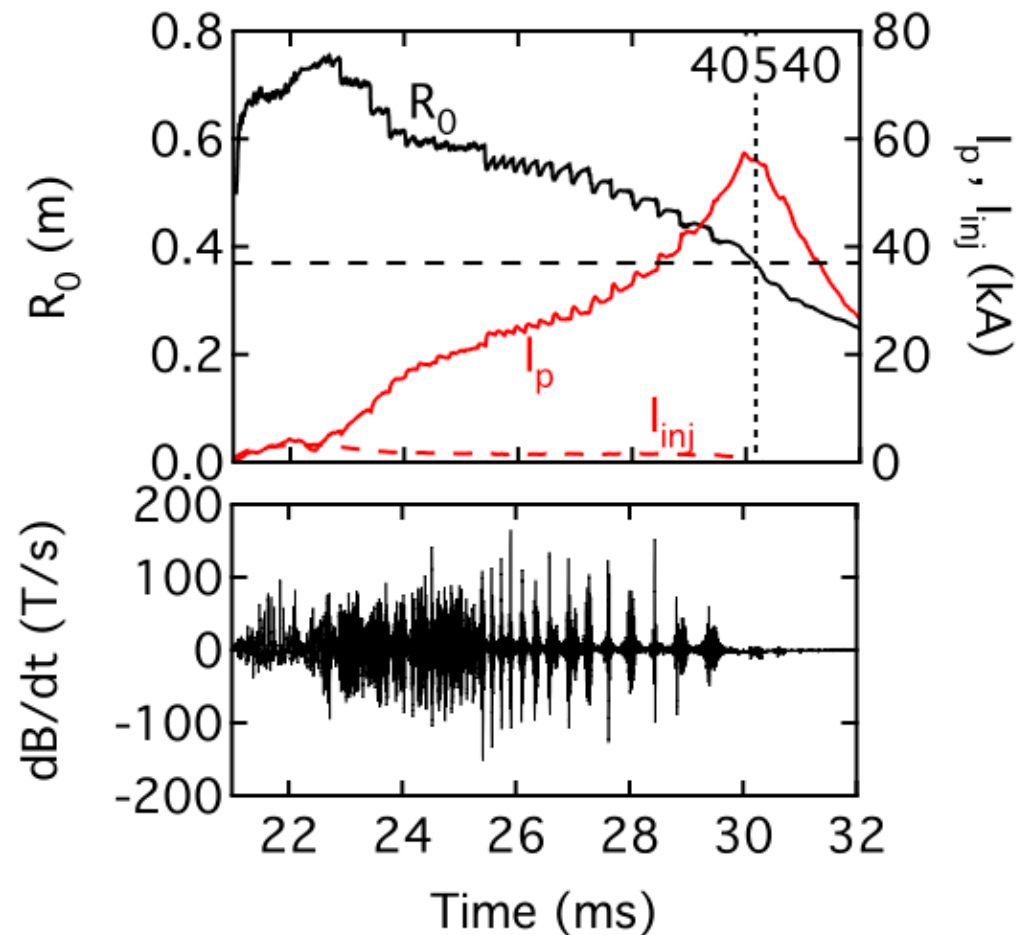
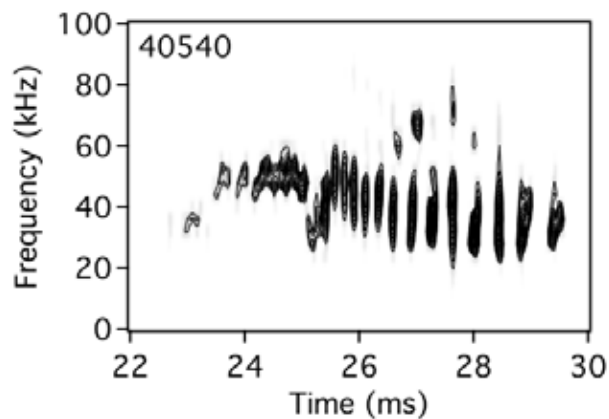
- Model evolving for source impedance  $\sim$  helicity injection rate
  - Predicative model requires edge density measurements
- Initiation phase: vacuum space charge limitation
  - $I_{\text{bias}} \sim V^{3/2} / d^2$
- High  $I_{\text{bias}}$  drive phase: expanding double layer sheath
  - $d^2 \sim V \Rightarrow I_{\text{bias}} \sim V^{1/2}$





# Intermittent 20 - 60 kHz $n = 1$ mode observed with strong edge current drive

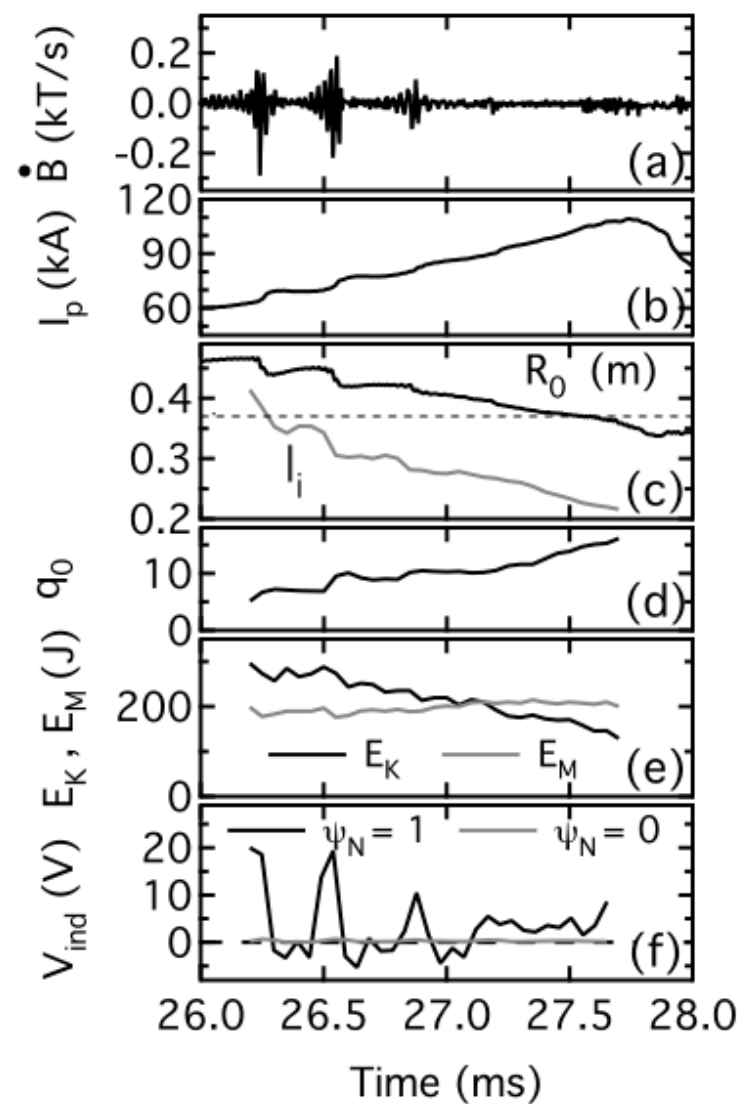
- Bursts of  $n = 1$  magnetic oscillations
  - Observed when plasma is coupled to edge current drive
  - Different in nature from inboard current injection experiments





# The magnetic topology quickly changes with each burst of MHD activity

- Each burst typically  $\sim 0.1$  ms
- With each burst...
  - $I_i$  decreases  $\rightarrow I_p$  increases
  - $R_o$  decreases  $\rightarrow$  plasma expands
  - $B_{\phi 0}$  increases  $\rightarrow q_o$  increases
  - Slight drop in  $E_k$  and  $E_m$
  - Very little change in poloidal flux at plasma edge
  - Rapid decrease in the total trapped poloidal flux



- Temporally and spatially averaged  $V_{ind} \sim 1.5$  V

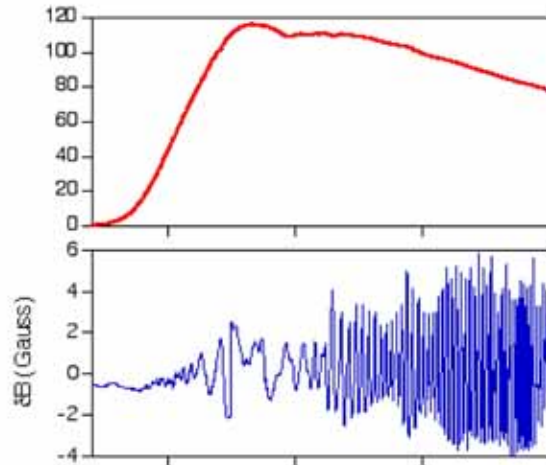




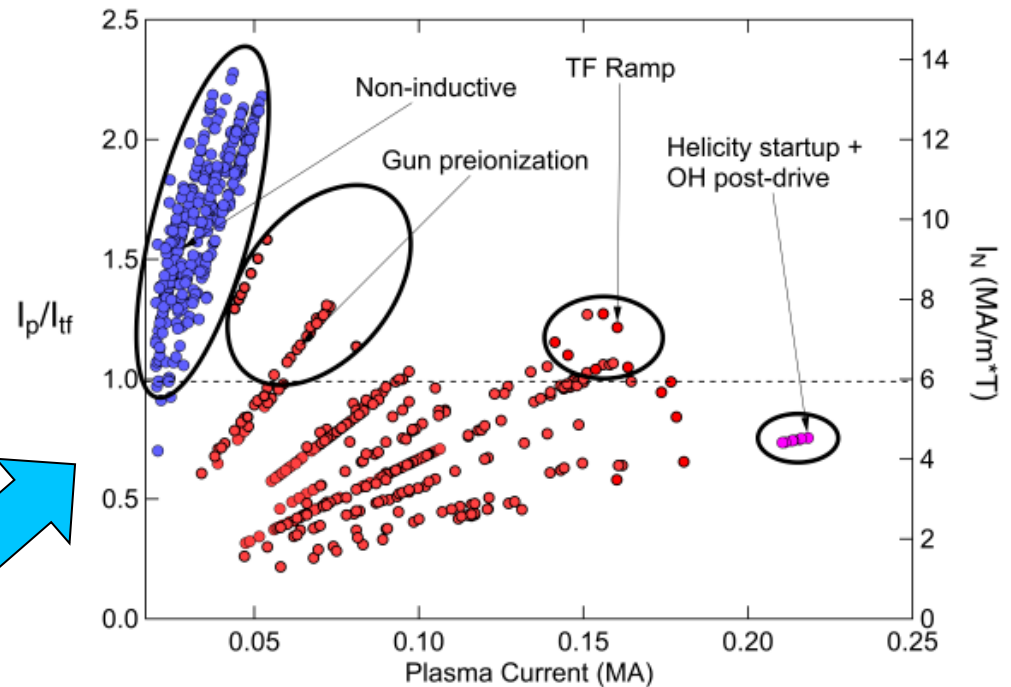
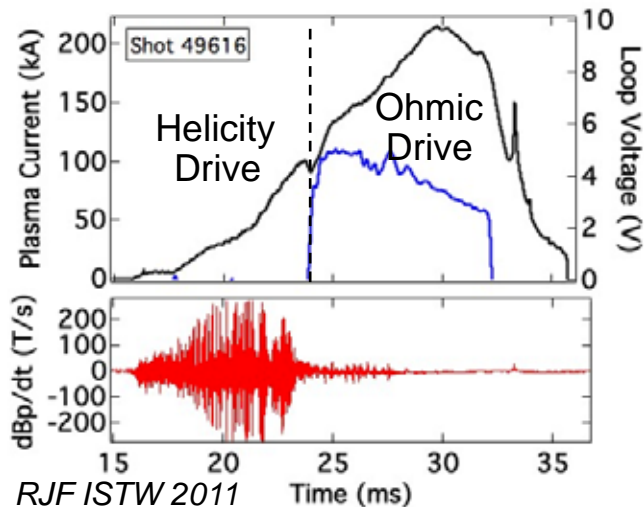


# Current Drive Tools Providing Access to High Field Utilization Regime

OH only = large 2/1 modes limit  $I_p$



HI startup = MHD quiescent

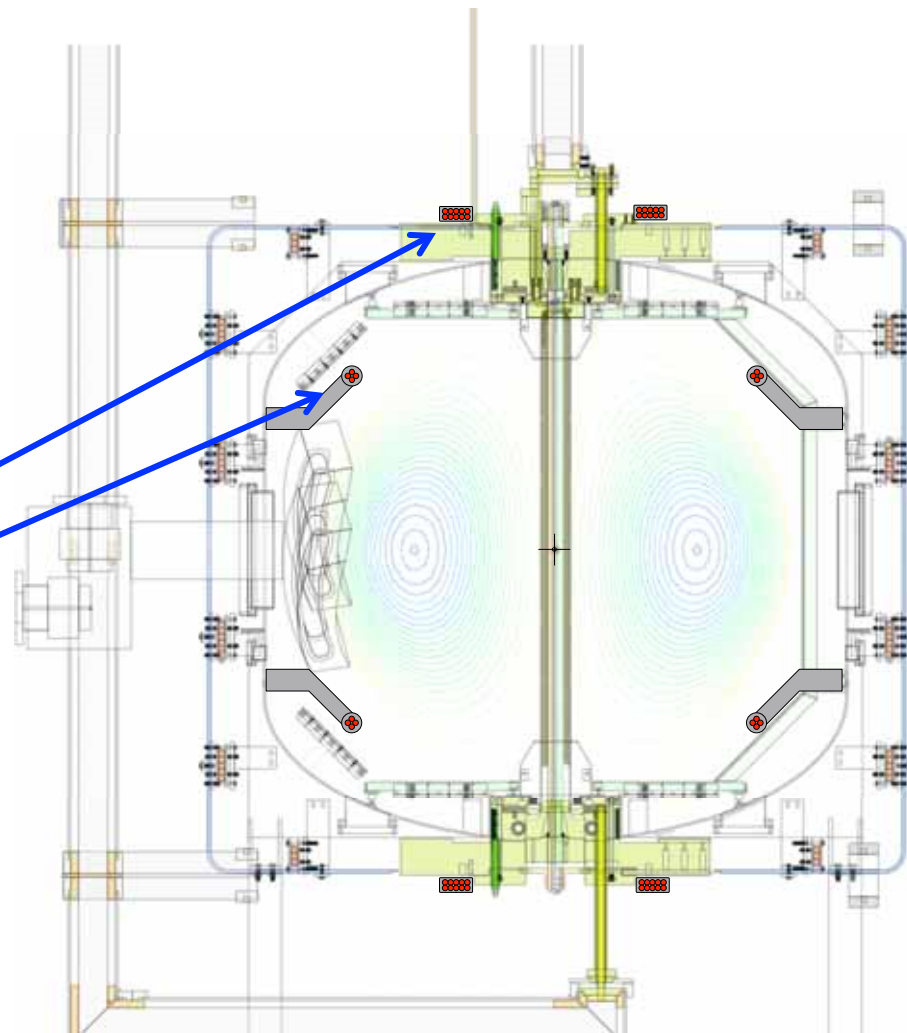


- Helicity injection startup and Ohmic sustainment provides MHD-stable profiles at  $I_p/I_{TF} < 1$
- Need to extend to higher  $I_p$ , then to low  $I_{TF}$  for high  $I_N$  and high  $\beta_T$  as  $A \approx 1$



# Medium-Term Upgrades Will Allow Further Tests of Point-Source Helicity Injection

- Gun-electrode Evolution
  - Passive electrode material variations
    - C electrode being installed
  - Separate plasma gun and electrode
- Power Supplies, Heating
  - New helicity injection power: 2 kV, 15 kA
  - Double TF current: *Taylor limit increase*
  - Commission HHFW system: *electron heating*
- Expanded PF Coil Set and control
  - Internal coils for radial position control
  - New external divertor coils
  - Implement GA Plasma Control System
- Diagnostic Additions
  - Multipoint Thomson Scattering
  - High-speed  $T_i(r,t)$ 
    - *Anomalous reconnection heating*

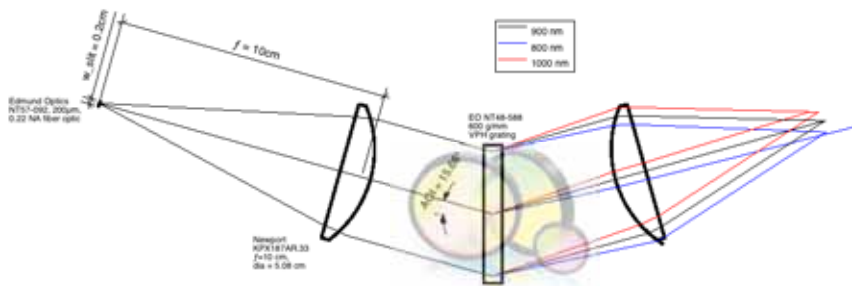




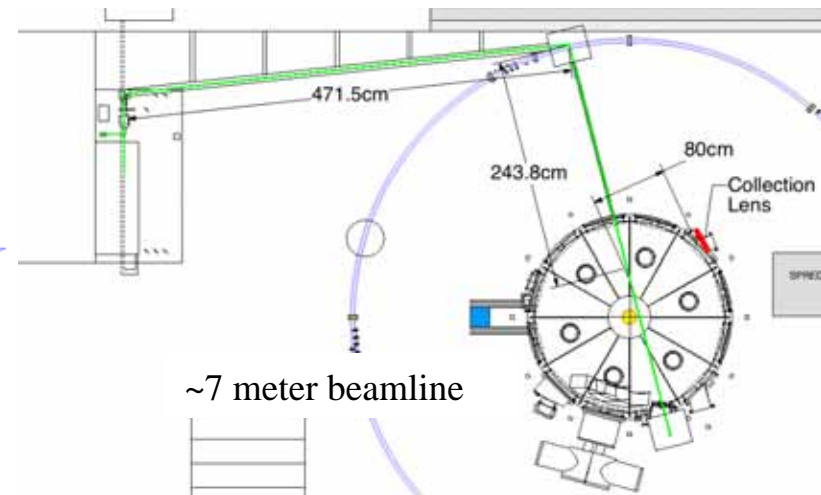
# Thomson Scattering system uses new technologies for visible wavelength system

- Frequency doubled Nd:YAG laser provides  $\sim 10^{18}$  photons
- For typical PEGASUS plasma,  $n_{\text{scattered}} \sim 10^4$  photons
- **VPH grating** efficiency  $> 85\%$  for  $\lambda_{\text{inc}} = 532 - 632$  nm
- **Gen III image intensifiers**  $\sim 50\%$  efficient in visible region
- $\sim 6$  ns ICCD gating provides easy detector technology

Laser Specifications	Value
Output Energy at 532 nm	$\geq 2000$ mJ
Beam diameter at head	12 mm
Beam diameter at waist	3 mm
Pointing stability	$\leq 50$ $\mu$ rad
Divergence	$\leq 0.5$ mrad
Repetition Rate	$\leq 10$ Hz
Pulse length	$\geq 10$ ns



Volume Phase Holographic (VPH) Grating





## HI Conclusion: High- $I_p$ Non-Solenoidal Startup via Point-Source Helicity Injection Looks Promising

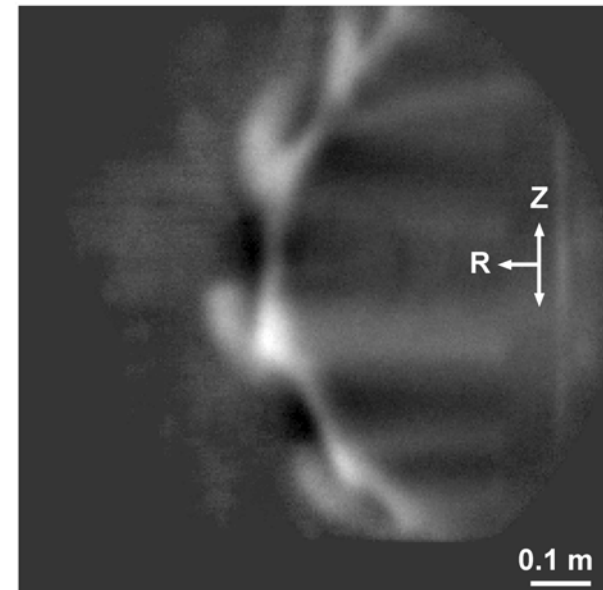
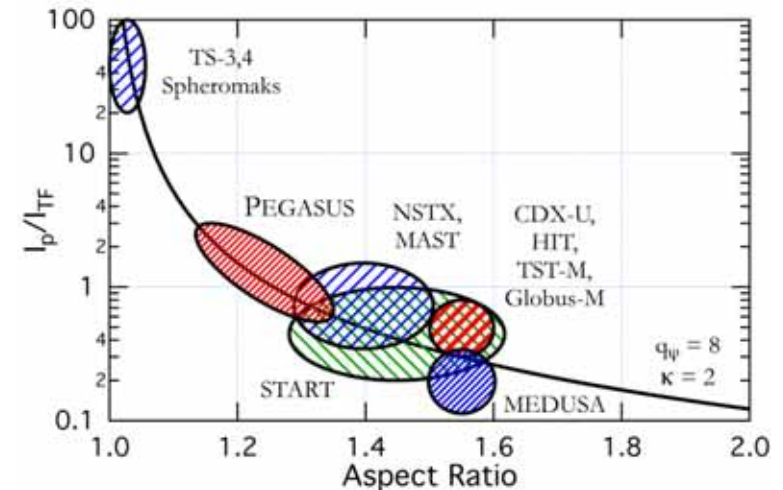
- Significant progress with non-solenoidal startup of ST
  - $I_p \sim 0.17$  MA using helicity injection and outer-PF rampup
  - Using understanding of helicity balance and relaxation current limit to guide hardware and operational changes
    - So far, predicted scalings supported
  - Goal  $\approx 0.3$ - $0.4$  MA non-solenoidal  $I_p$  to extrapolate to next level/NSTX
    - Outstanding physics questions:  $\lambda_{\text{edge}}$ ,  $Z_{\text{inj}}$ , confinement, *etc.*
  - Deploying plasma diagnostics to better understand properties
- Exploration of high  $I_N$ ,  $\beta_t$  space facilitated by  $j(r)$  tools
  - $I_p/I_{\text{TF}} > 2$ ,  $I_N > 14$  achieved; extend operation to high  $I_p$ ,  $n_e$  for high  $\beta_t$
- Holds Promise as a Scalable Non-Inductive Startup Technique
  - Simpler injection system using plasma gun – passive electrode combination may be feasible





# Some Low-A ST ITER-relevance: Access to Peeling Instability and Conditions to Measure $J$

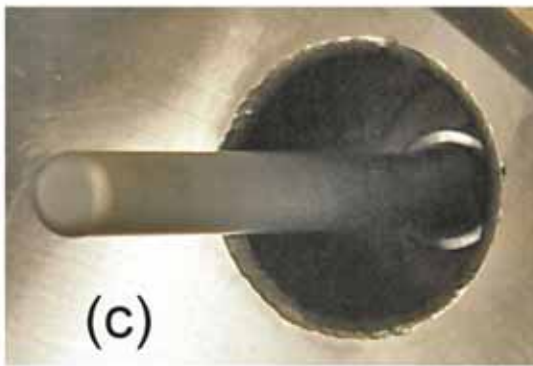
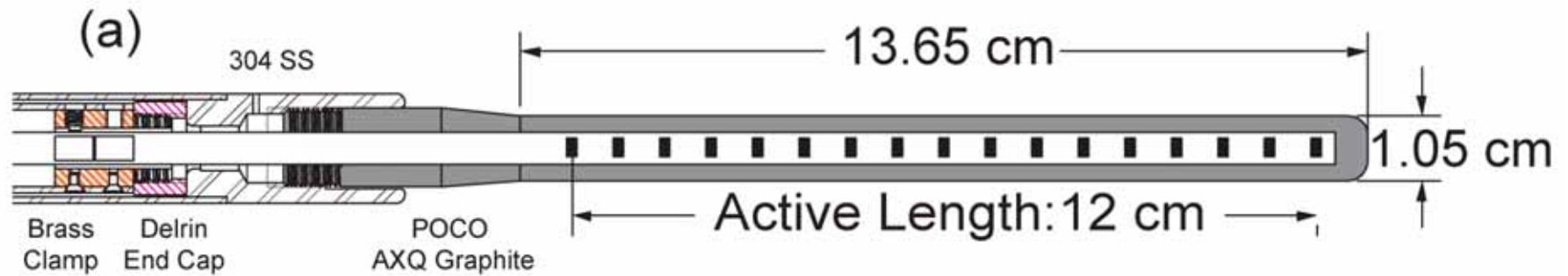
- Spherical tokamaks naturally provide strong peeling drive
  - Toroidal field utilization  $I_p/I_{TF} \sim j_{||}/B$
- PEGASUS accesses peeling modes
  - Strong  $j_{||}/B$  MA/m<sup>2</sup>-T at
  - Comparable to DIII-D in H-mode
- Machine parameters permit internal edge measurements
  - Short pulse lengths (< 50 ms)
  - Modest  $T_e < 200$  eV



Bongard *et al.*, Phys. Rev. Lett. **107**, 035003 (2011)



# PEGASUS Hall Probe Deployed to Measure J



- Solid-state InSb Hall sensors
  - Sypris model SH-410
- Slim C armor as low-Z PFC
  - Minimizes plasma perturbation
- 16 channels, 7.5 mm radial resolution
- 25 kHz bandwidth



## $J_\phi(R,t)$ Calculable Directly from Ampère's Law

$$\mu_0 J_\phi = (\nabla \times \mathbf{B})_\phi = \frac{\partial B_R}{\partial Z} - \frac{\partial B_Z}{\partial R}$$

- Simplest test follows from  $B_R(Z)$  or  $B_Z(R)$  measurements
- Petty\* solves for an off-midplane  $B_Z(R)$  measurement set and an elliptical plasma cross-section:

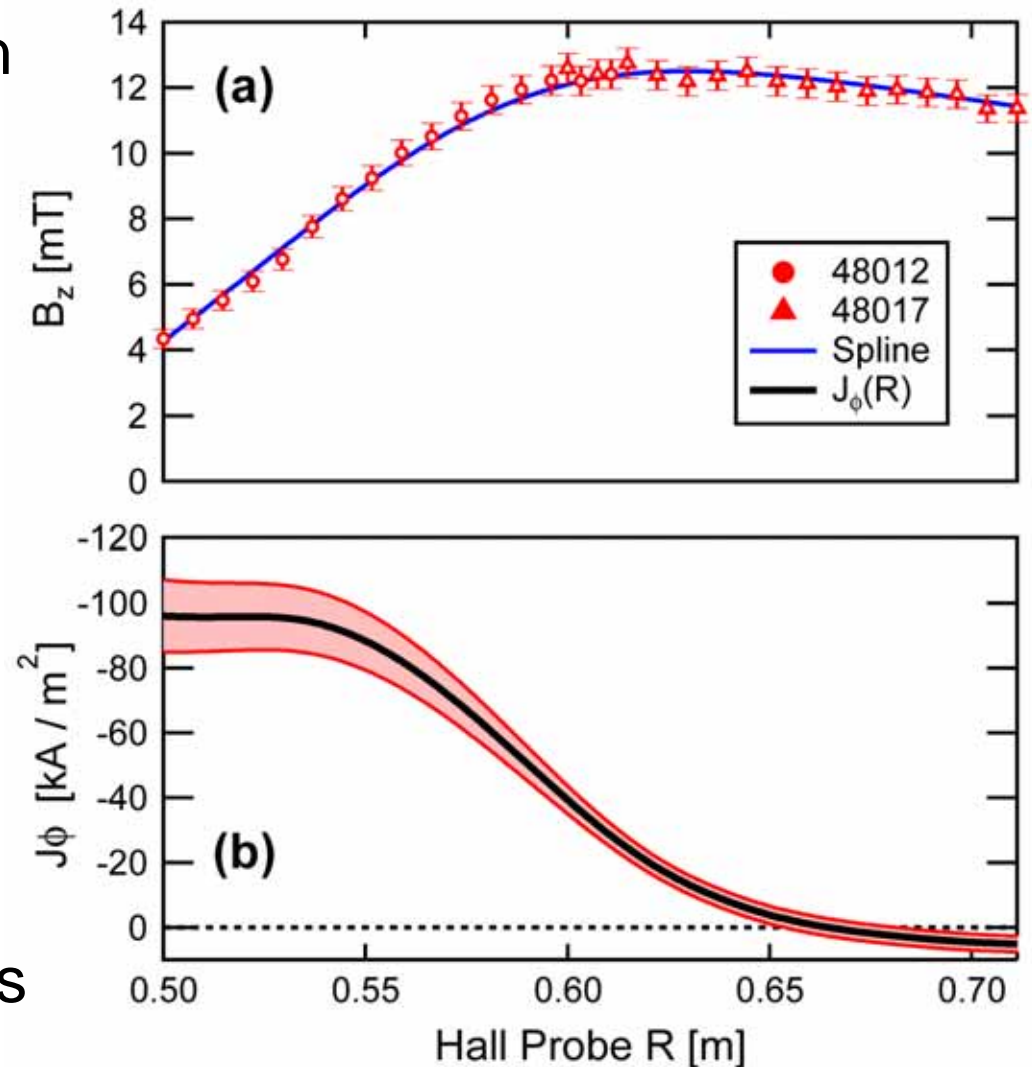
$$\mu_0 J_\phi = -\frac{B_Z}{\kappa^2 (R - R_0)} \left( 1 - \frac{Z^2 R_0}{\kappa^2 R (R - R_0)^2} \right) - \frac{dB_Z}{dR} \left( 1 + \frac{Z^2}{\kappa^4 (R - R_0)^2} \right)$$

- Does not make assumptions on shape of  $J(R)$



# Direct $J_\phi(R)$ Profiles Obtained in PEGASUS

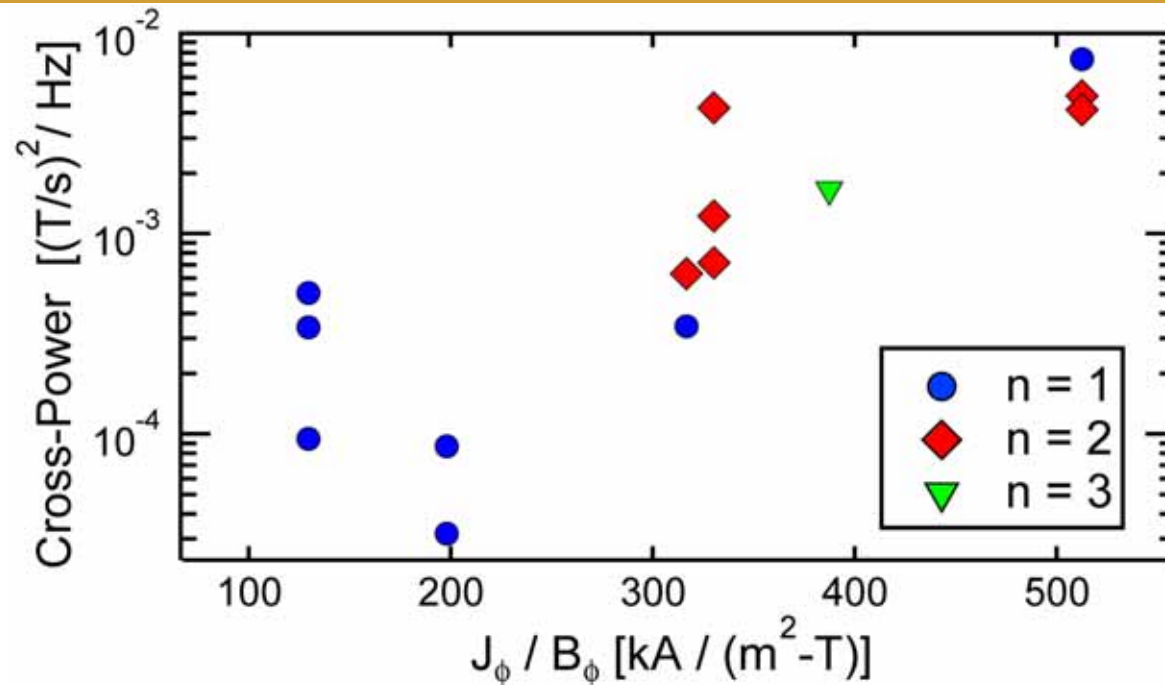
- Straightforward J estimation
  - Obtain Hall Probe  $B_z(R,t)$
  - Compute  $dB_z/dR$  using interpolated smoothing spline\*
  - Compute  $J_\phi(R,t)$  given geometry
- Resultant  $J_\phi(R,t)$  consistent with  $I_p$ , MHD evolution
- Radial span extendible with multi-shot averaging
- Higher-order shaping effects negligible within errors



Bongard *et al.*, Phys. Rev. Lett. **107**, 035003 (2011)



# Peeling MHD Strongly Scales with Theoretical Drive



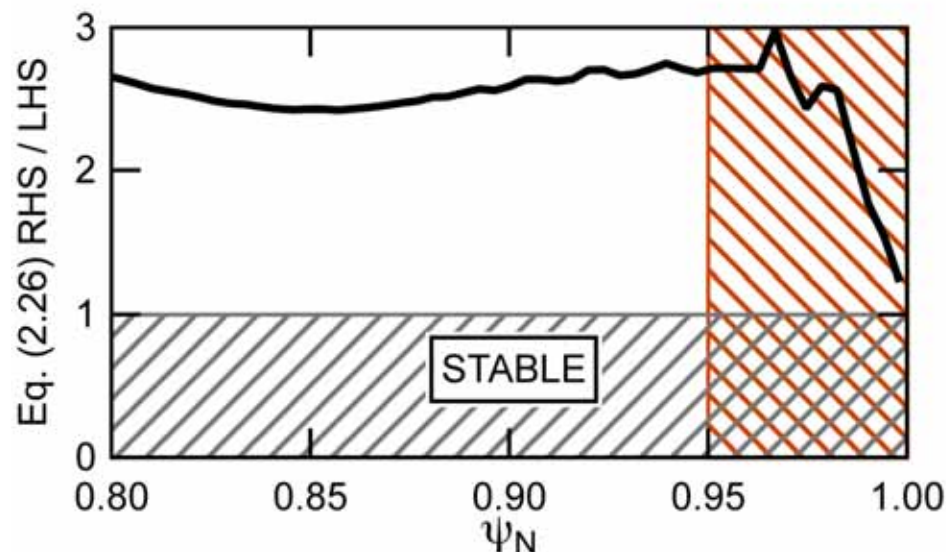
- Mode helicities estimated from port 8 Mirnov array
  - $n < 3$  via cross-phase analysis
  - $m_{\text{lab}} \geq 10$  via radial decay rate
  - $10 \leq m_{\text{lab}} / n \leq 30$  ( $\psi \downarrow N > 0.9$ )
- MHD power spans two orders of magnitude with factor-of-five variation in J/B



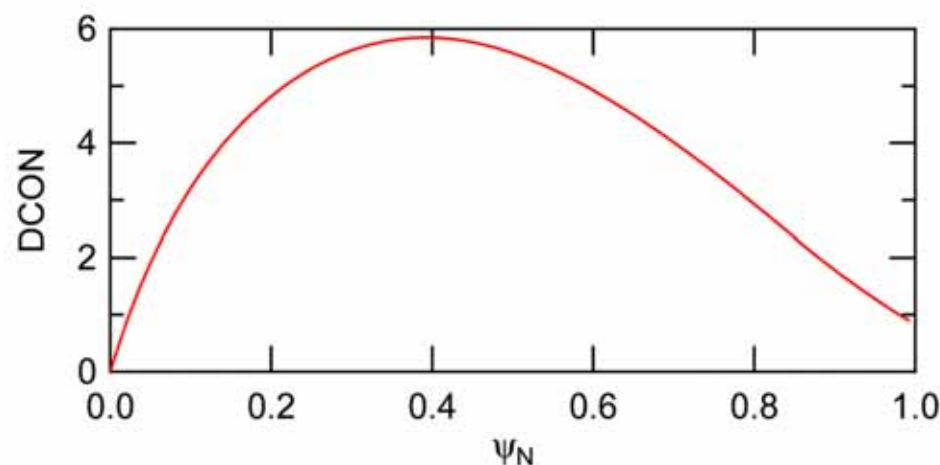


# Stability Analysis Confirms Peeling Instability

- Analytic peeling criterion computed from Hall-constrained equilibrium indicates instability
  - More than factor of two in region of optimal  $\langle J \downarrow \phi \rangle$  constraint
- Free-boundary ideal stability analysis performed with DCON
  - Indicates instability to  $m/n = 19/1$  external kink
- Both methods agree with experiment



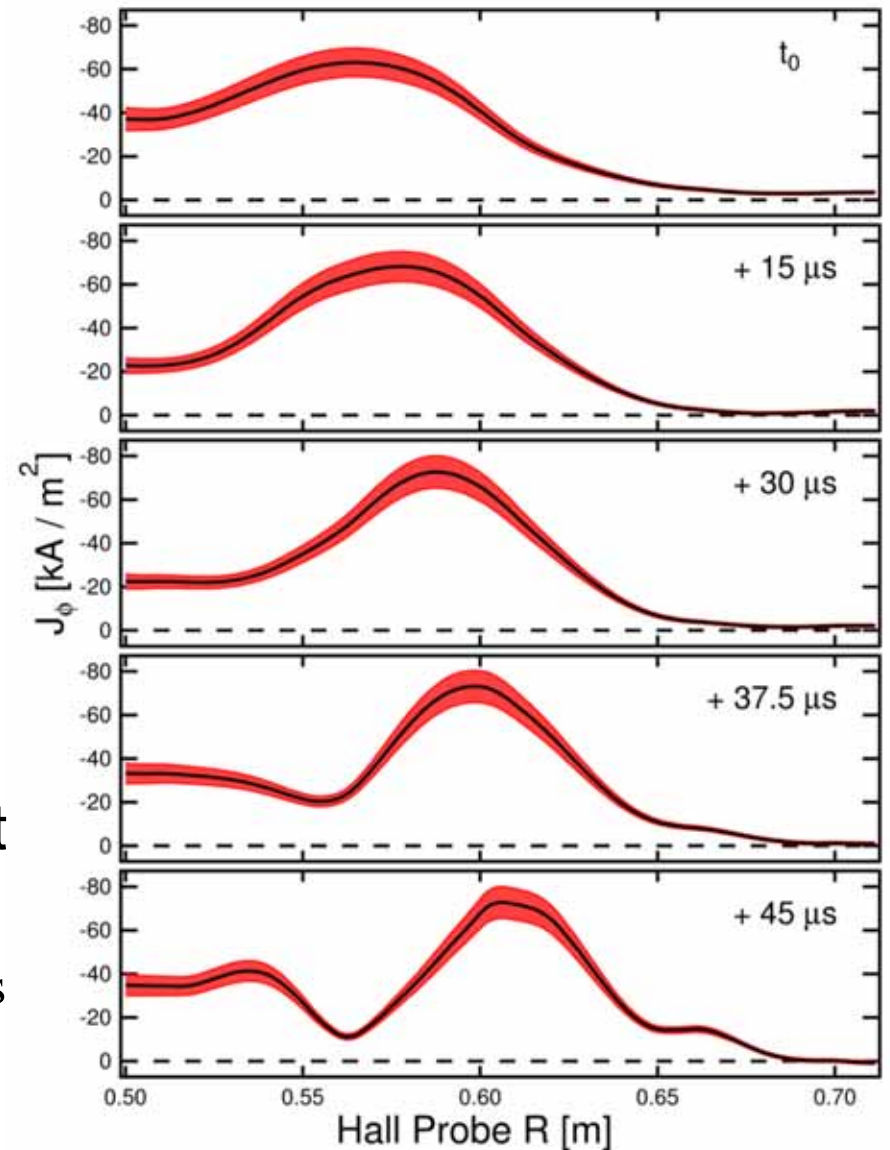
Bongard *et al.*, Phys. Rev. Lett. **107**, 035003 (2011)





# $J_{\text{edge}}$ Dynamics Measured on ELM Timescales

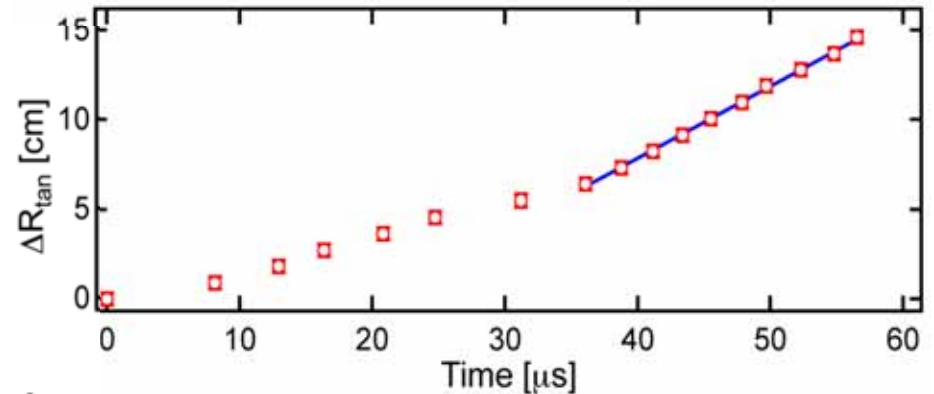
- $J_{\text{edge}}$  resolved during peeling filament generation
- Propagating filament forms from initial “current-hole”  $J_{\text{edge}}$  perturbation
  - Validates formation mechanism hypothesized by EM blob transport theory
- Filament carries toroidal current  $I_f \sim 100\text{--}220\text{ A}$ 
  - Comparable to MAST ELM estimates
  - $I_f < 0.2\%$  of  $I_p$



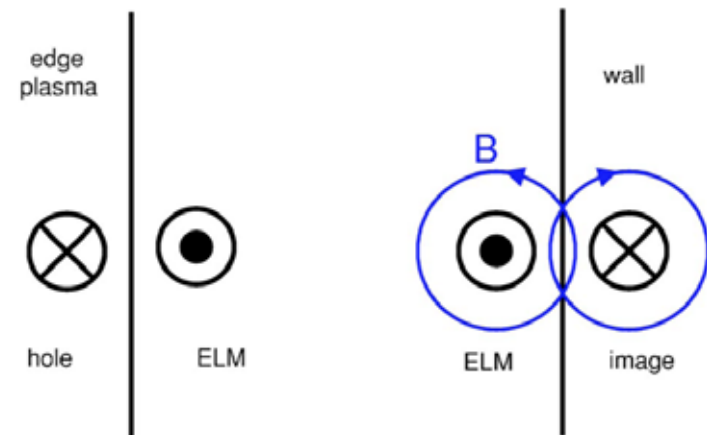
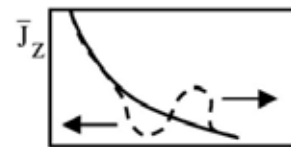


# Filament Radial Motion Qualitatively Consistent with Electromagnetic Blob Transport

- Trajectory of detached filament tracked with 275 kHz imaging
  - Radially accelerates, followed by constant velocity motion
- Magnetostatic repulsion\* plausibly contributes to dynamics
  - Current-hole  $\mathbf{J} \times \mathbf{B}$  drives  $aR$
  - Transition at  $\sim 35 \mu\text{s}$  comparable to healing time of current-hole
- Measured  $VR$  comparable to available EM blob models\*\*
  - $VR \sim 4 \text{ km/s}$ ;  $VR, IB \sim 8 \text{ km/s}$
  - Agrees to  $O(1)$  accuracy of theory



Bongard *et al.*, Phys. Rev. Lett. **107**, 035003 (2011)



\*: Myra, Phys. Plasmas **14**, 102314 (2007)

\*\* : Myra *et al.*, Phys. Plasmas **12**, 092511 (2005)



# Peeling Mode / ELM Conclusions

- Direct measurements of  $J_{\text{edge}}$  conducted with Hall probe
  - Direct analysis, equilibrium reconstruction
  - $J_{\text{edge}}$  controllable with  $dI_p/dt$
- Characteristics of Peeling Modes Consistent with Theory
  - Macroscopic features: Low- $n$ , high- $m$  external kink
  - Onset consistent with ideal MHD, analytic peeling stability theories
  - Observed MHD scales with measured  $J/B$  peeling drive
  - Coherent, propagating filaments
- $J_{\text{edge}}$  dynamics supports current-hole & EM blob hypotheses
  - Nonlinear filaments generated from current-hole  $J_{\text{edge}}$  perturbation
  - Transient magnetostatic repulsion
  - Constant- $V_R$  propagation in agreement with available EM blob theory





# HI Conclusion: High- $I_p$ Non-Solenoidal Startup via Point-Source Helicity Injection Looks Promising

- Significant progress with non-solenoidal startup of ST
  - $I_p \sim 0.17$  MA using helicity injection and outer-PF rampup
  - Using understanding of helicity balance and relaxation current limit to guide hardware and operational changes
    - So far, predicted scalings supported
  - Goal  $\approx 0.3$ - $0.4$  MA non-solenoidal  $I_p$  to extrapolate to next level/NSTX
    - Outstanding physics questions:  $\lambda_{\text{edge}}$ ,  $Z_{\text{inj}}$ , confinement, *etc.*
  - Deploying plasma diagnostics to better understand properties
- Exploration of high  $I_N$ ,  $\beta_t$  space facilitated by  $j(r)$  tools
  - $I_p/I_{\text{TF}} > 2$ ,  $I_N > 14$  achieved; extend operation to high  $I_p$ ,  $n_e$  for high  $\beta_t$
- Holds Promise as a Scalable Non-Inductive Startup Technique
  - Simpler injection system using plasma gun – passive electrode combination may be feasible



# Plasma Startup via Local Helicity Injection and Stability Studies at Near-Unity Aspect Ratio in the Pegasus Experiment

R.J. Fonck, J.L. Barr, M.W. Bongard, M.G. Burke,  
E.T. Hinson, A.J. Redd, N. Schoenberg,  
D.J. Schlossberg, K.E. Thome

*The Joint Meeting of 5th IAEA Technical Meeting on Spherical Tori*

*16th International Workshop on Spherical Torus (ISTW2011)*

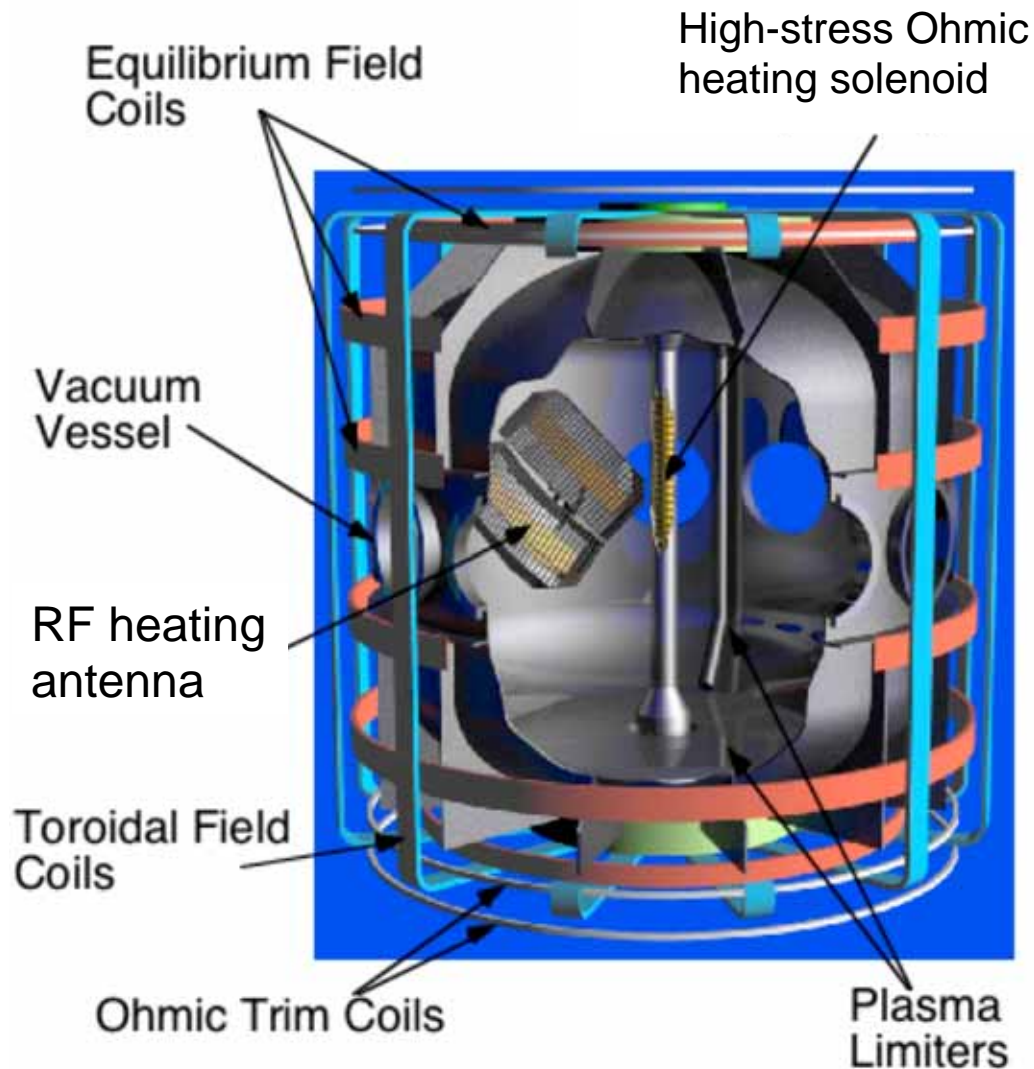
*2011 US-Japan Workshop on ST Plasma*

*National Institute for Fusion Science, Toki, Japan September 27-30, 2011*





# PEGASUS is a Compact Ultralow-A ST



## Experimental Parameters

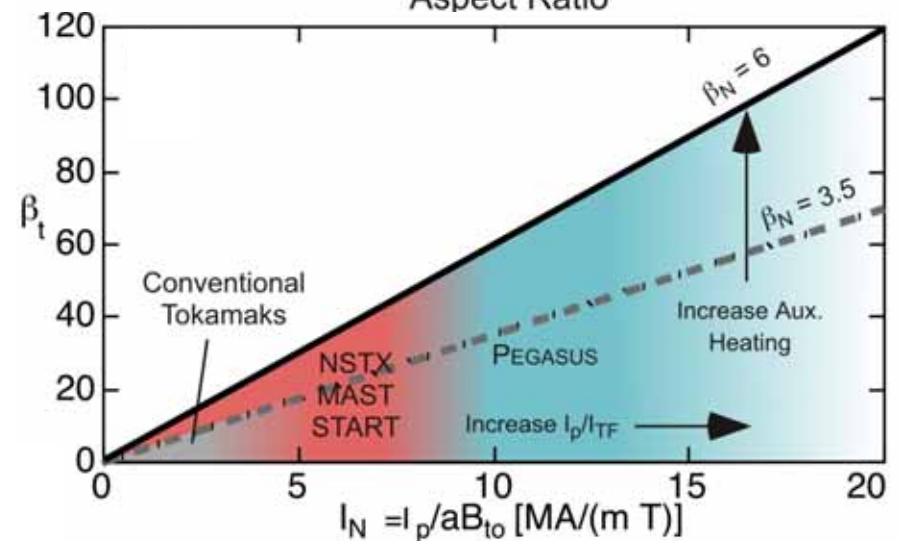
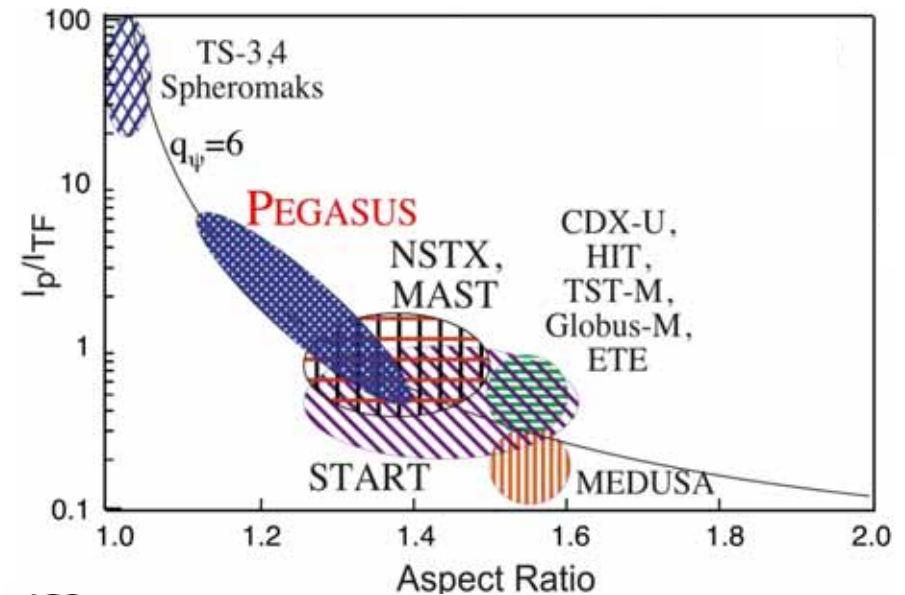
<u>Parameter</u>	<u>To Date</u>
A	1.15 – 1.3
R(m)	0.2 – 0.45
$I_p$ (MA)	$\leq .22$
$I_N$ (MA/m-T)	6 – 12
$l_i$	0.2 – 0.5
$\kappa$	1.4 – 3.0
$\tau_{\text{shot}}$ (s)	$\leq 0.025$
$\beta_T$ (%)	$\leq 25$
$P_{\text{HHFW}}$ (MW)	0.2





# PEGASUS Mission: Physics of Low $A \rightarrow 1$

- University-scale, Low-A ST
  - $R_0 \leq 0.45$  m,  $a \sim 0.40$  m
- Physics of High  $I_p/I_{TF}$ 
  - Expand operating space of the ST
  - Study high  $\beta_T$  plasmas as  $A \rightarrow 1$
- Non-solenoidal startup
  - Point-source helicity injection
  - Helicity injection discharges couple to other current drive methods
- Peeling-mode studies
  - Experimental tests of peeling-ballooning theory (ELM, ITER)

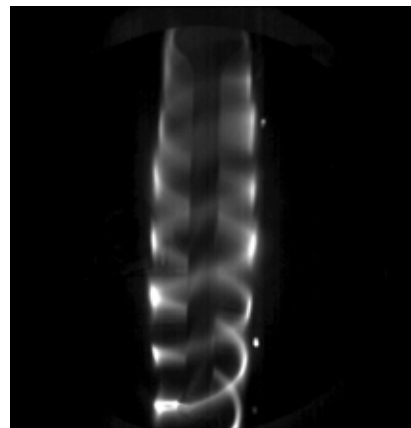






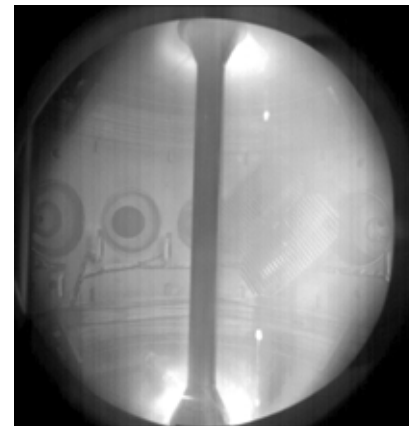
## Local Plasma Current Sources + Helical Vacuum Field Give Simple DC Helicity Injection Scheme

- Current is injected into the existing helical magnetic field
- High  $I_{inj}$  & modest  $B \Rightarrow$  filaments merge into current sheet
- High  $I_{inj}$  & low  $B \Rightarrow$  current-driven  $B_\theta$  overwhelms vacuum  $B_z$ 
  - Relaxation via MHD activity to tokamak-like Taylor state w/ high toroidal current multiplication



Current filaments

Reduced  $B_z$   
→



Relaxed tokamak

- Technical attractiveness: can remove sources and anode after startup





# DC Helicity Injection Startup on PEGASUS Utilizes Localized Washer-Gun Current Sources

- Plasma gun(s) biased relative to anode:

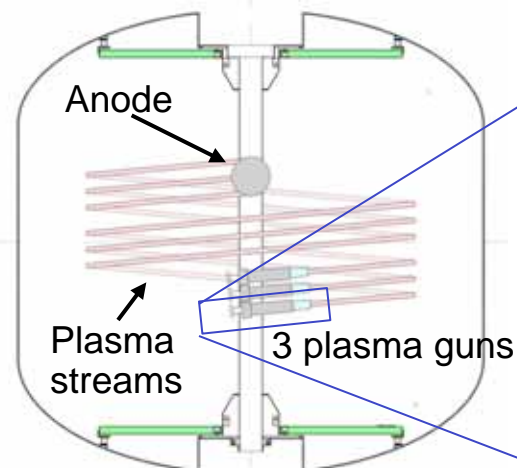
- Helicity injection rate:

$$\dot{K}_{inj} = 2V_{inj}B_N A_{inj}$$

$V_{inj}$  - injector voltage

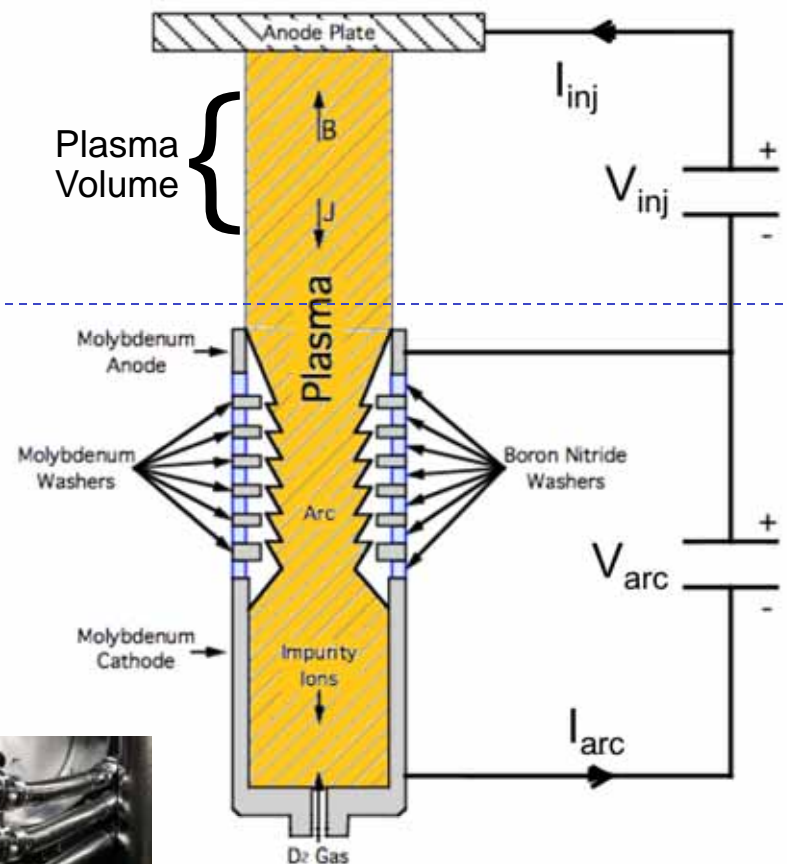
$B_N$  - normal B field at gun aperture

$A_{inj}$  - injector area



Midplane Injection

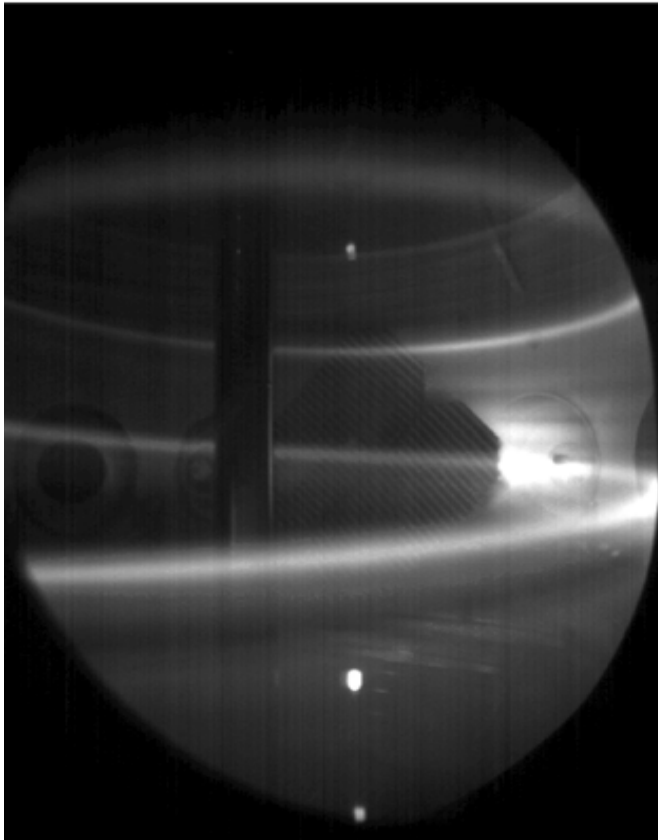
Simplified illustration of a plasma gun for helicity injection  
(not to scale)



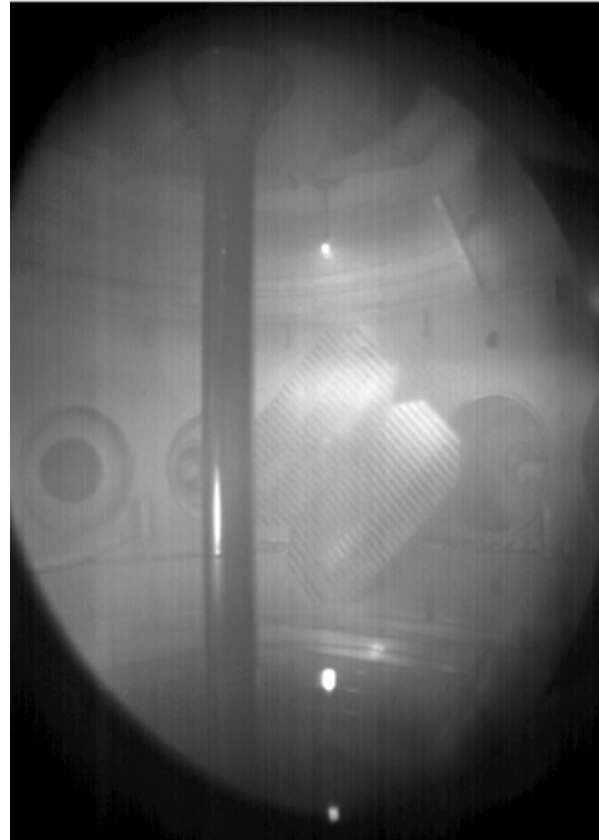


# Evolution of midplane-gun-driven plasma

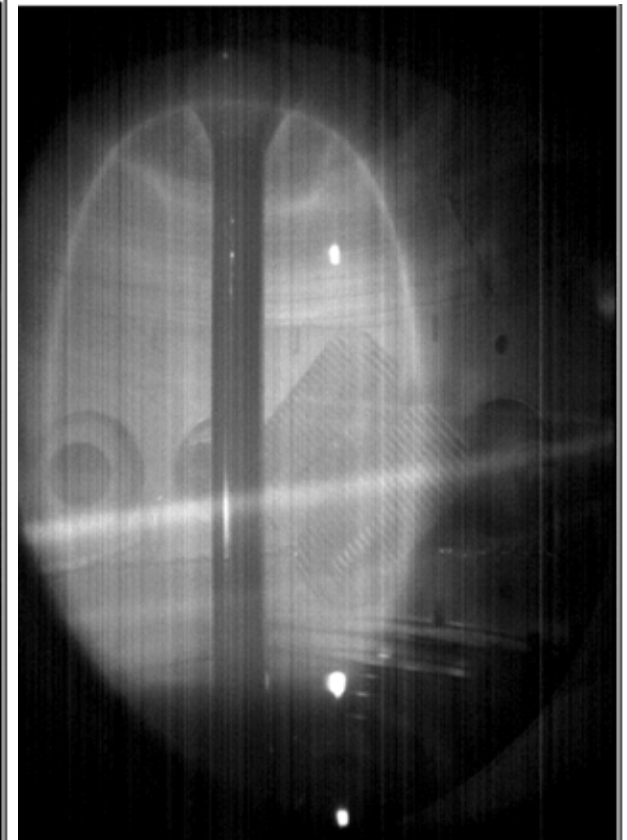
PEGASUS shot #40458: two midplane guns, mild outer-PF ramp



$t=21.1$  ms,  $I_p=2-3$  kA  
Filaments only



$t=28.8$  ms,  $I_p=42$  kA  
Driven diffuse plasma



$t=30.6$  ms,  $I_p=37$  kA  
Guns off, Decaying



# Taylor Relaxation Criteria Sets the Maximum $I_p$ for a Given Magnetic Geometry

Helicity balance in a tokamak geometry:

$$\frac{dK}{dt} = -2 \int_V \eta \mathbf{J} \cdot \mathbf{B} d^3x - 2 \frac{\partial \Psi}{\partial t} \Psi - 2 \int_A \Phi \mathbf{B} \cdot d\mathbf{s} \quad \longrightarrow \quad I_p \leq \frac{A_p}{2\pi R_0 \langle \eta \rangle} (V_{ind} + V_{eff})$$

- Helicity injection can be expressed as an effective loop voltage
- $I_p$  limit depends on the scaling of plasma confinement via the  $\eta$  term

$$V_{eff} \approx \frac{A_{inj} B_{\phi, inj}}{\Psi_T} V_{bias}$$

Taylor relaxation of a force-free equilibrium:

$$\begin{aligned} \nabla \times \mathbf{B} = \mu_0 \mathbf{J} = \lambda \mathbf{B} \\ \lambda_p \leq \lambda_{edge} \end{aligned} \quad \longrightarrow \quad \frac{\mu_0 I_p}{\Psi_T} \leq \frac{\mu_0 I_{inj}}{2\pi R_{inj} w B_{\theta, inj}} \quad \longrightarrow \quad I_p \leq \left[ \frac{C_p}{2\pi R_{inj} \mu_0} \frac{\Psi_T I_{inj}}{w} \right]^{1/2}$$

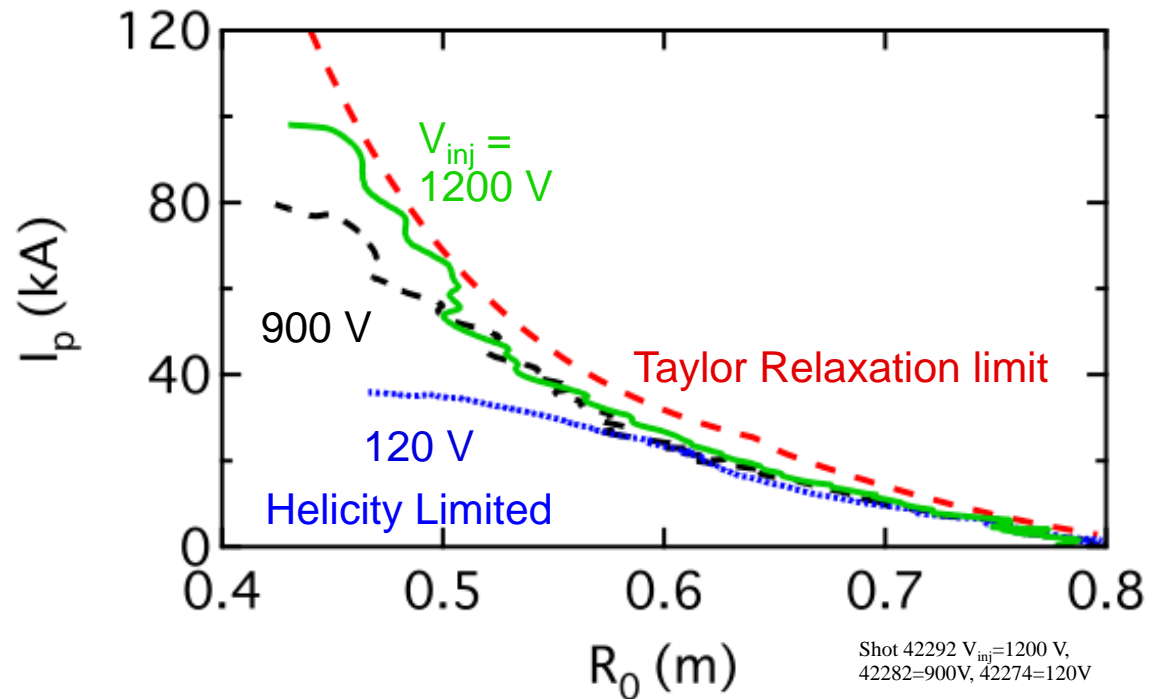
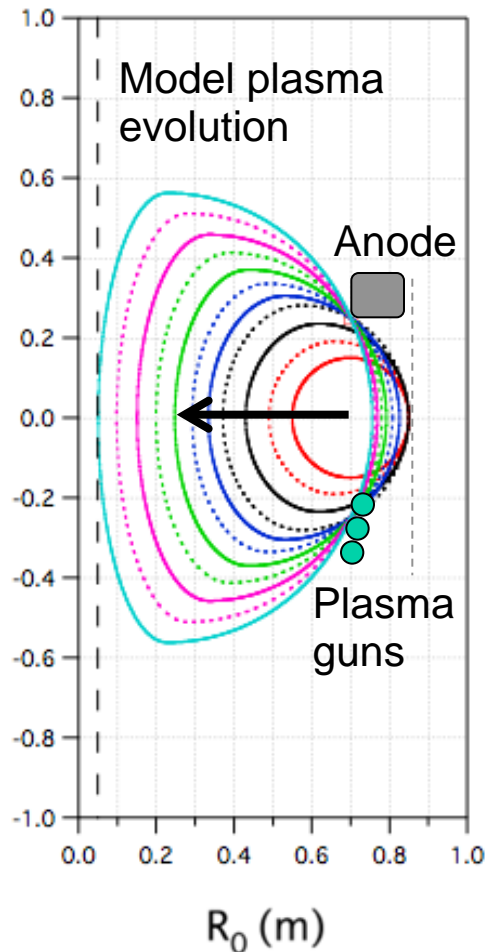
Assumptions:

- Driven edge current mixes uniformly in SOL
- Edge fields average to tokamak-like structure

$A_p$	Plasma area
$C_p$	Plasma circumference
$\Psi_T$	Plasma toroidal flux
$w$	Edge current channel width



# Achieving the Maximum $I_p$ at the Taylor Limit Requires Sufficient Helicity Injection Input Rate



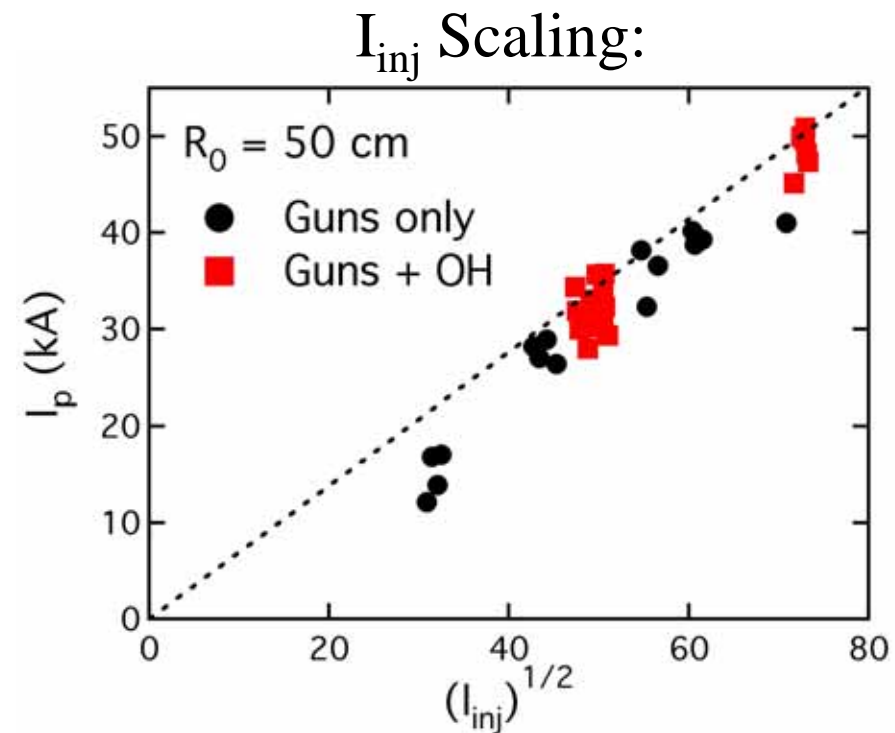
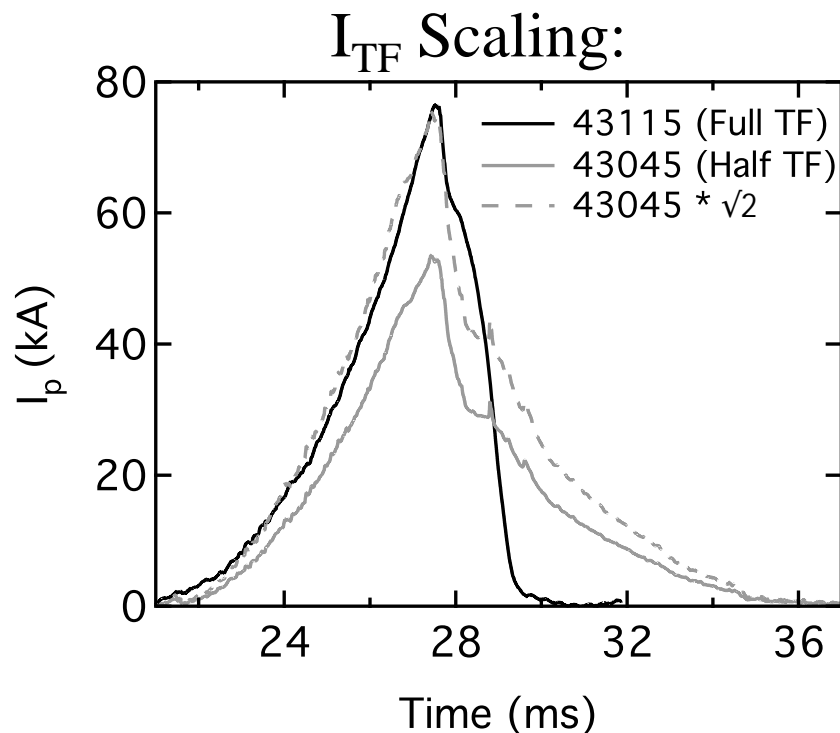
- Helicity input rate, and effective net volt-seconds, increases as  $V_{inj}$  increases
- Sufficient net V-sec needed to reach Taylor relaxation limit





# Experiments Confirm Relaxation Limit Scalings with $I_{TF}$ and $I_{inj}$

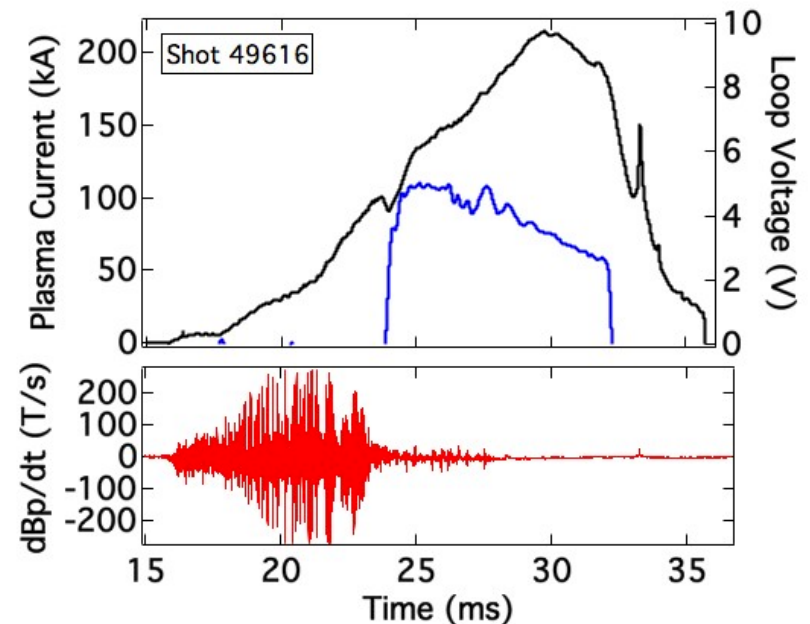
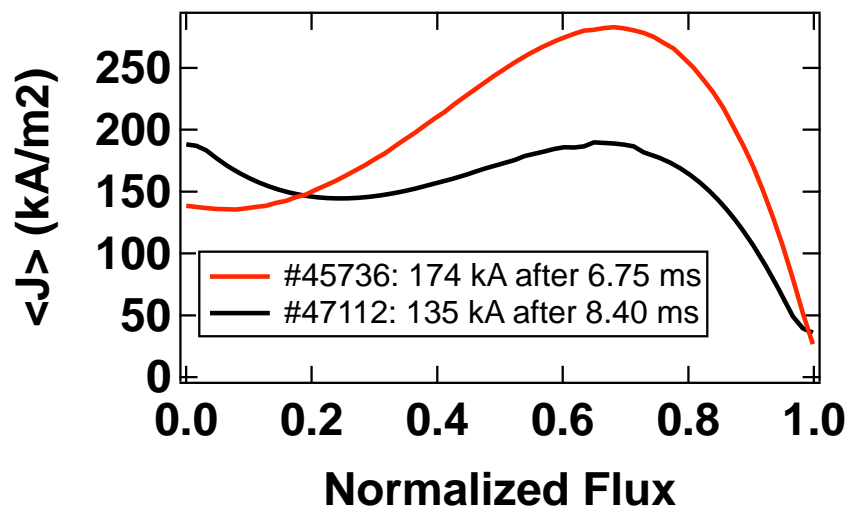
- The relaxation limit  $I_p$  scales with: 
$$I_p \propto \left[ \frac{I_{TF} I_{inj}}{W} \right]^{1/2}$$
- Experimental plasma current limits follow these scalings:





# Slowly-evolving Gun-driven Plasmas Hand Off Most Efficiently to Ohmic Drive

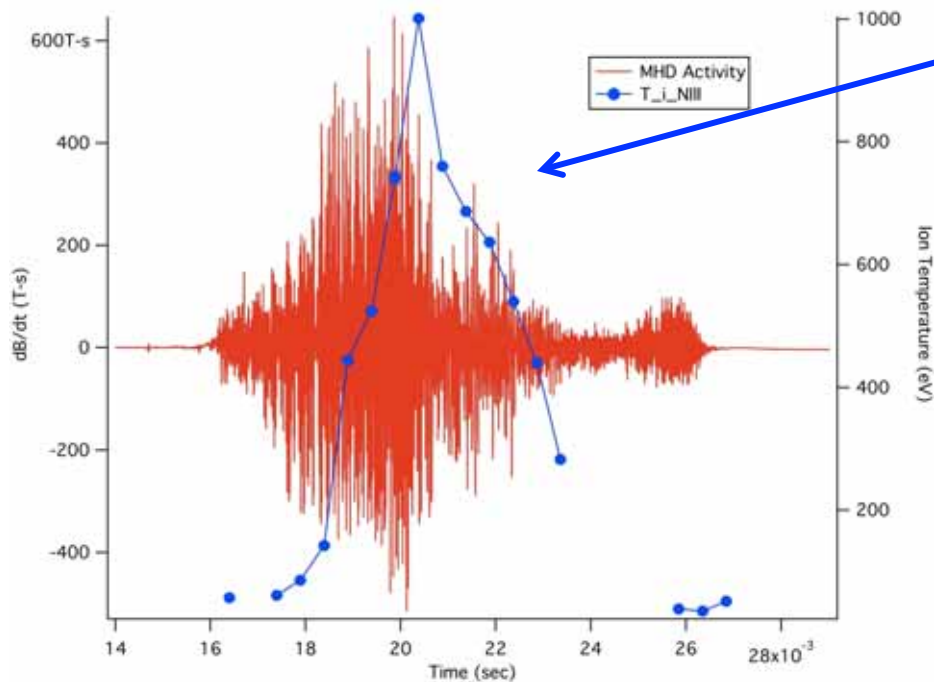
- Poloidal flux generated by helicity injection is equivalent to that generated by Ohmic Drive
  - $I_{\text{total}} = I_{\text{HI}} + I_{\text{OH}}$
- Excessive skin current  $\Rightarrow$  poor coupling to OH drive
- Slowly evolving:  $\sim$  flat  $j(r)$  (black)
  - Smooth handoff to Ohmic inductive drive ( $j(R)$  profiles from external-only equilibrium reconstructions;  $l_i < 0.3$ )
- Rapidly evolving:  $\sim$  hollow, strong skin  $j(r)$  (red)
  - Does not hand off efficiently to Ohmic drive





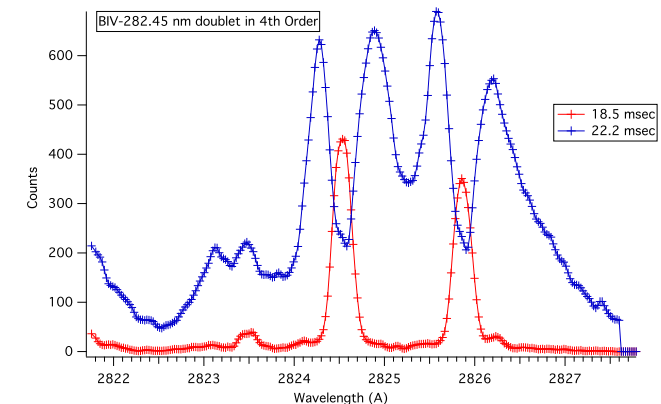
# Initial Spectroscopy Measurements Suggest Energetic Ions

- Spectroscopic  $T_i$  suggest high ion energies during reconnection period



Doppler  $T_i$  from radial view

Complex multi-line structures from tangential view



- However, situation is much more complex if viewed toroidally
  - Need improved time-resolution and spatial scans



# Several Issues to Address for a Predictive Model

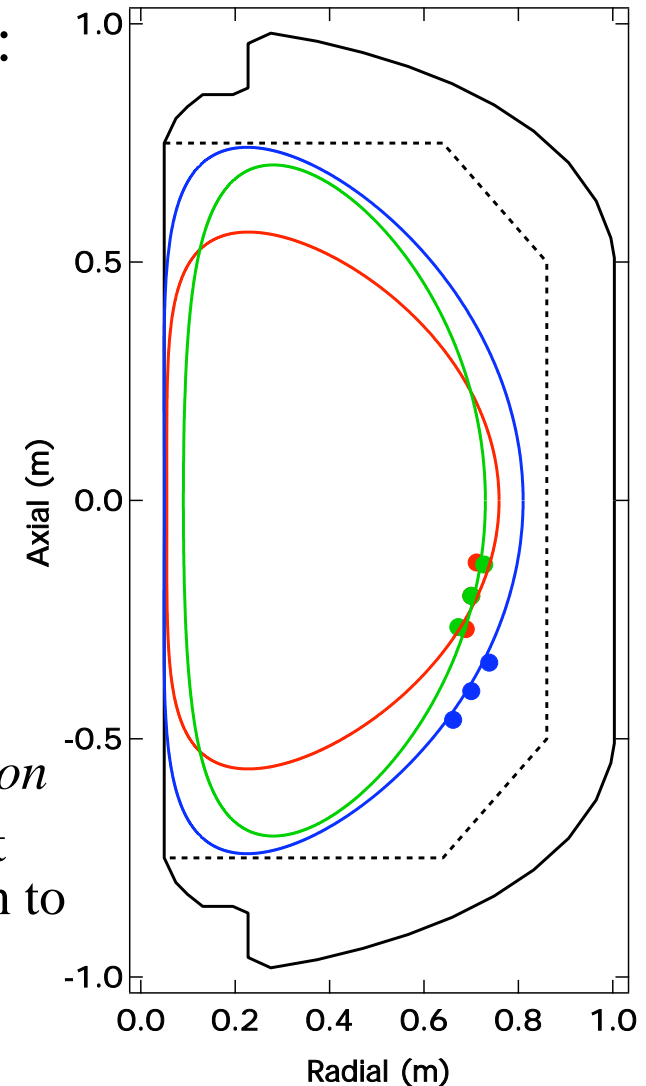
- Extension to higher current, longer pulse
  - Verify limit scalings
  - Discharge evolution for long growth phase
  - Test confinement properties, especially  $T_e(r,t)$ 
    - Helicity dissipation scaling model
- Optimal gun-electrode configuration
- Increased helicity injection rate
  - Test regime where helicity drive dominates PF induction for growth
  - Active guns vs. passive electrode approach for long-pulse growth
- Injected current source impedance model
  - What sets helicity injection rate?
- Edge  $j(r)$  measurements and  $\lambda(\psi,t)$ 
  - Physics of ultimate relaxation limits
  - Current transport: MHD behavior
- Impurity assessment and control





# Gun-Electrode Geometry: PF Induction, Plasma Size, and Null Formation

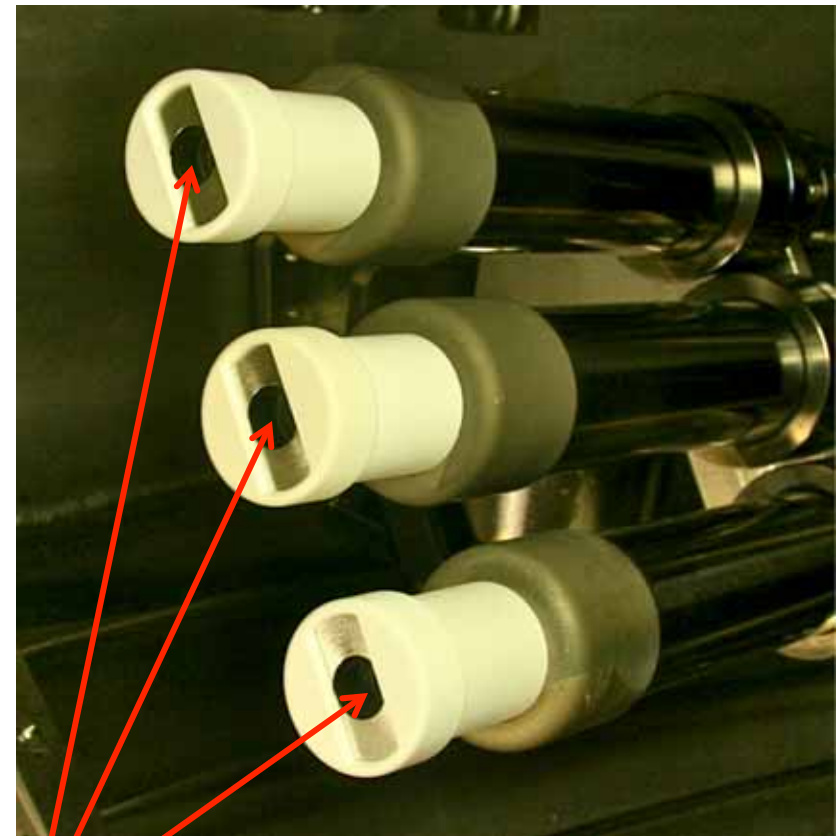
- Original: array was nearly vertical (red):
  - $J_{\text{edge}}$  width  $w$  scaled with # of guns
  - Maximum  $I_p = 0.11$  MA.
- Aligned gun array tilt (green):
  - Maximum  $I_p = 0.17$  MA.
  - 3-fold reduction in  $w$ ., consistent with changing the projected width at midplane.
- Maximize plasma size: array moved further away from midplane (blue):
  - Maximum  $I_p \sim 0.13$  MA
  - Larger startup plasma = *reduced PF induction*
  - *Poorer poloidal field null* formed by current streams = more difficult to induce relaxation to tokamak state
- Tight gun-anode geometry preferred





# Active Gun / Passive Electrode Assembly Points to Simpler, Higher $I_p$ Operation

- Potential for much higher  $I_{inj}$  without need for either more plasma guns or larger guns.
- Helicity injection physics is agnostic to the exact source of the edge charge carriers.
- Passive electrodes allow arbitrary shaping:
  - Can optimize both helicity input (large cross-sectional area) *and* the Taylor limit on  $I_p$  (narrow in radial direction)

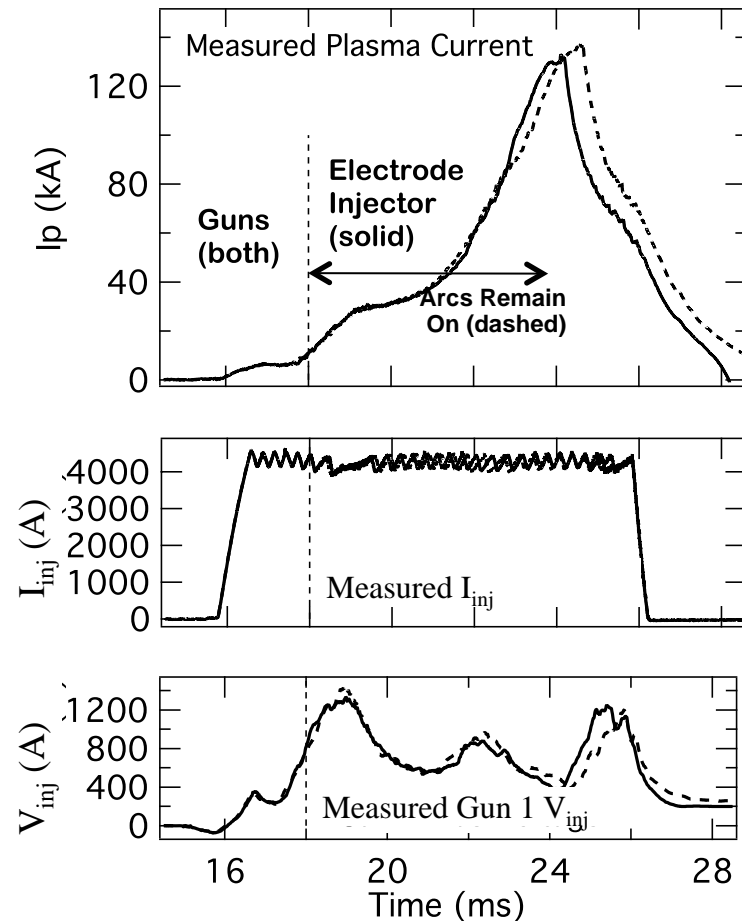


Plasma Guns with Integrated Slotted Electrodes



# Initial Tests of Gun/Electrode Helicity Injection System Are Promising

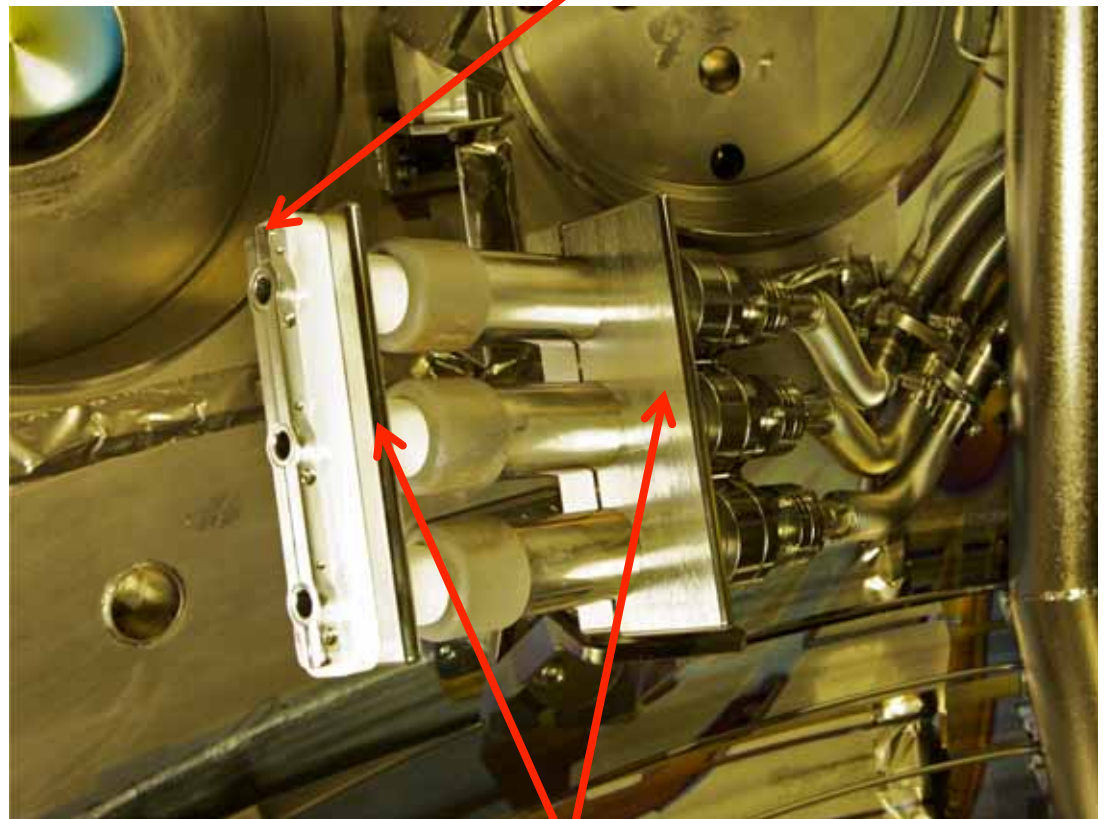
- Operations use two steps:
  - 1. Form initial tokamak-like state with minimal active arc gun
  - 2. Grow to much larger  $I_p$  with passive electrodes fed by electrode charge carriers induced and moderated by tokamak edge plasma.
- First tests are promising
  - Arc current off after relaxation and formation of tokamak-like state
  - $I_p$  rise is virtually the *same*, whether arc discharge or passive electrode provide the charge carriers





# Integrated Arc Gun – Passive Electrode Experiments Begun

- New gun-electrode assembly has extended electrode coupled to arc gun exit cathodes
  - Offers 5-times increase in helicity injection rate
- Integrated scraper limiters to protect assembly and control local edge density
  - Gas-puff control of  $V_{\text{bias}} \sim V_{\text{loop, effective}}$



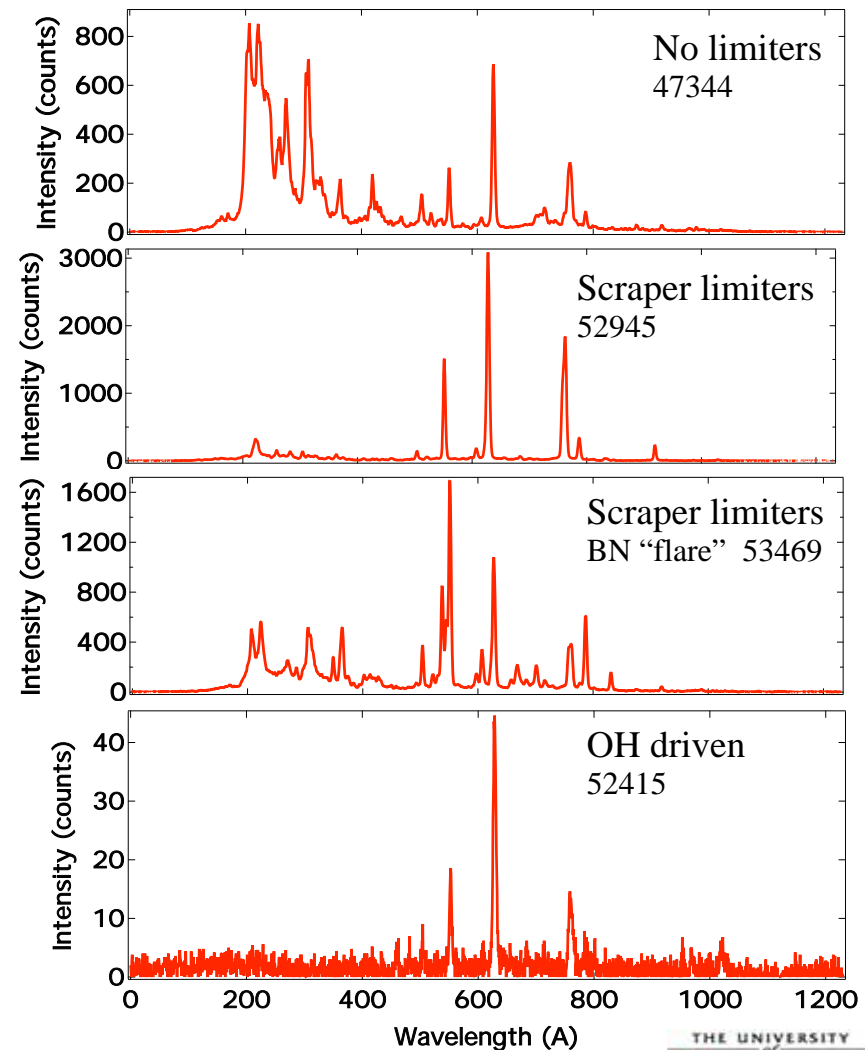
*Local limiters*





# Local Limiters Reduce N to Negligible Levels in Well-behaved Injection Cases

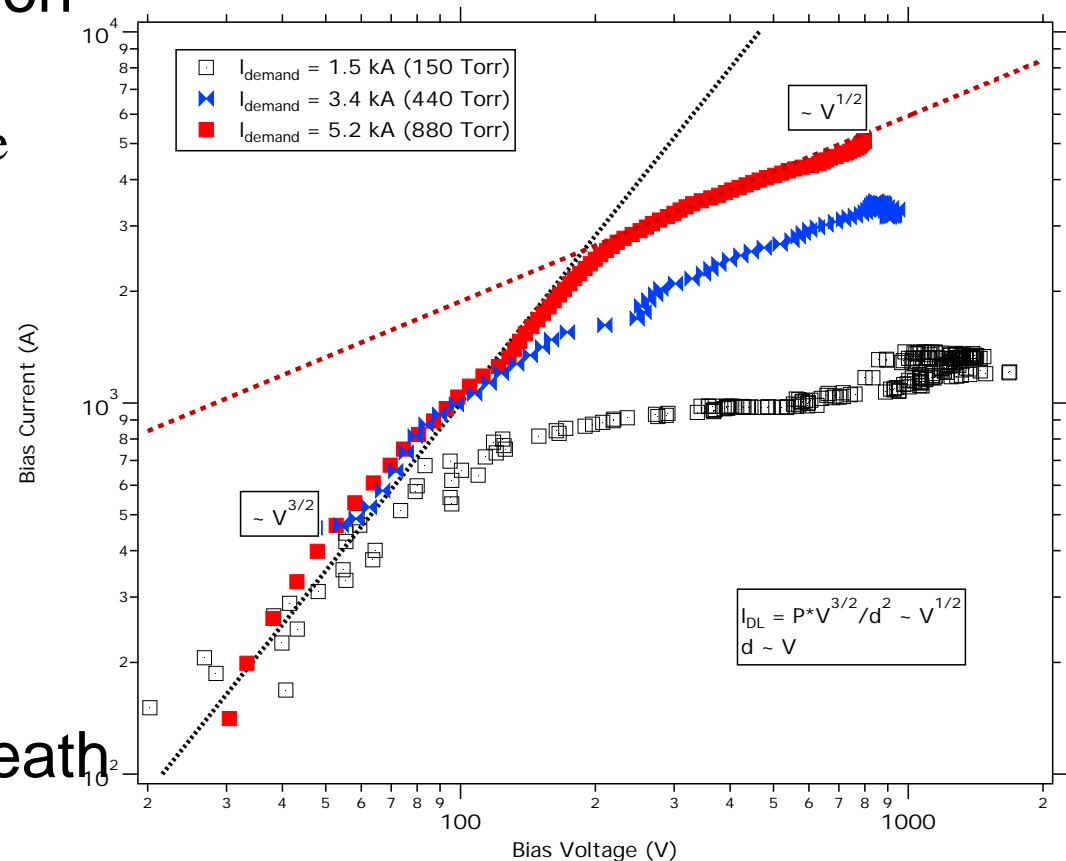
- N dominant impurity with unprotected gun assembly
  - 1<sup>st</sup> *estimates* of impurity content via bolometer measures
    - $Z_{\text{eff}} \sim 2.2. \pm 0.8$  during injection;  $\leq 1.4$  after injection
    - Mainly N;  $n_e \sim 5 \times 10^{18} \text{ m}^{-3}$  to  $2 \times 10^{19} \text{ m}^{-3}$
- Local scraper limiters much reduce N, O remains
- Bursts of N still evident with flare at BN surface
- Ohmic-only reference plasma very clean
  - $Z_{\text{eff}} \leq 1.2$





# Source Impedance Appears to be Governed by Sheath Physics

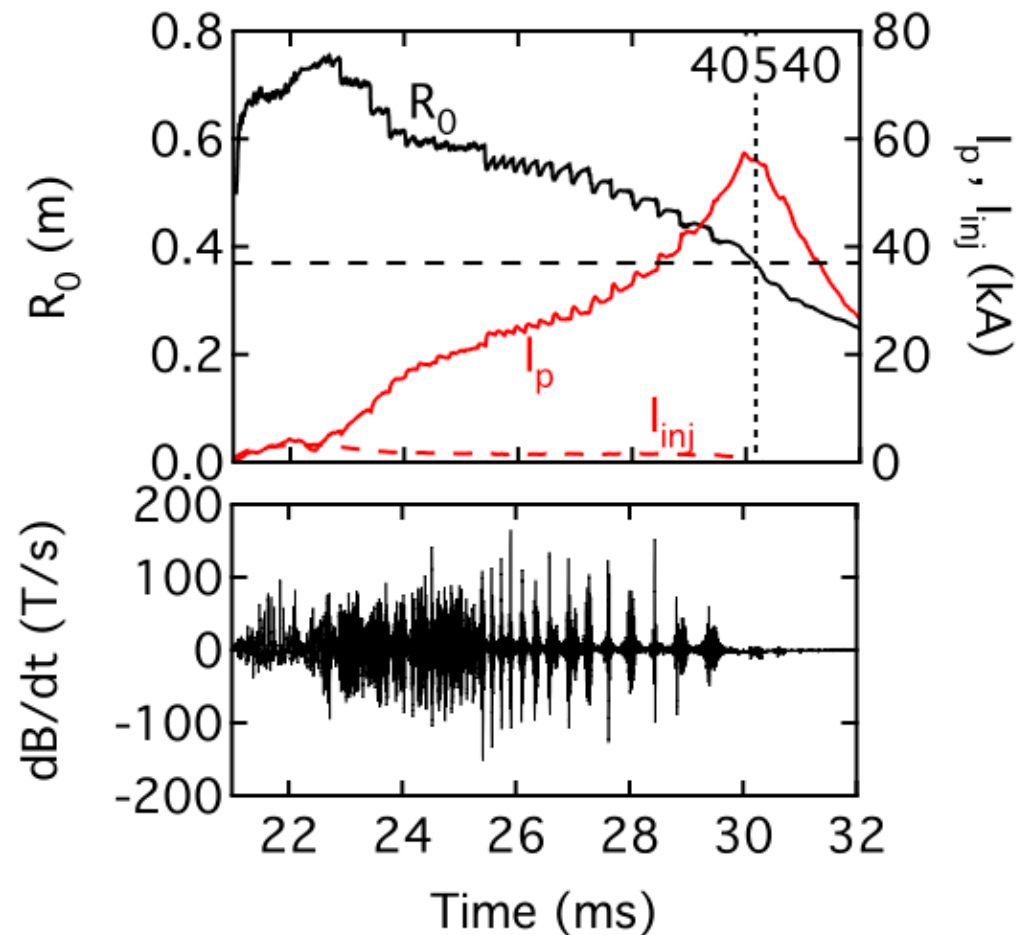
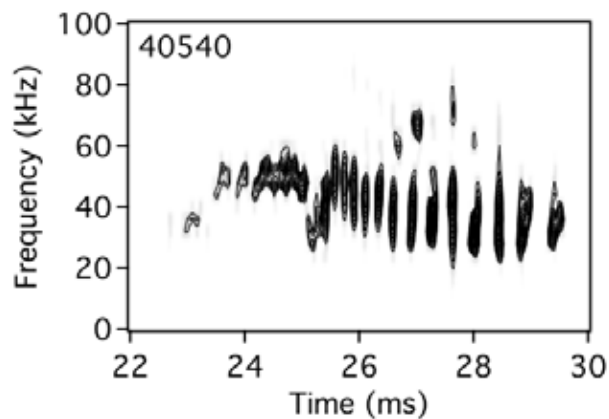
- Model evolving for source impedance  $\sim$  helicity injection rate
  - Predicative model requires edge density measurements
- Initiation phase: vacuum space charge limitation
  - $I_{\text{bias}} \sim V^{3/2} / d^2$
- High  $I_{\text{bias}}$  drive phase: expanding double layer sheath
  - $d^2 \sim V \Rightarrow I_{\text{bias}} \sim V^{1/2}$





# Intermittent 20 - 60 kHz $n = 1$ mode observed with strong edge current drive

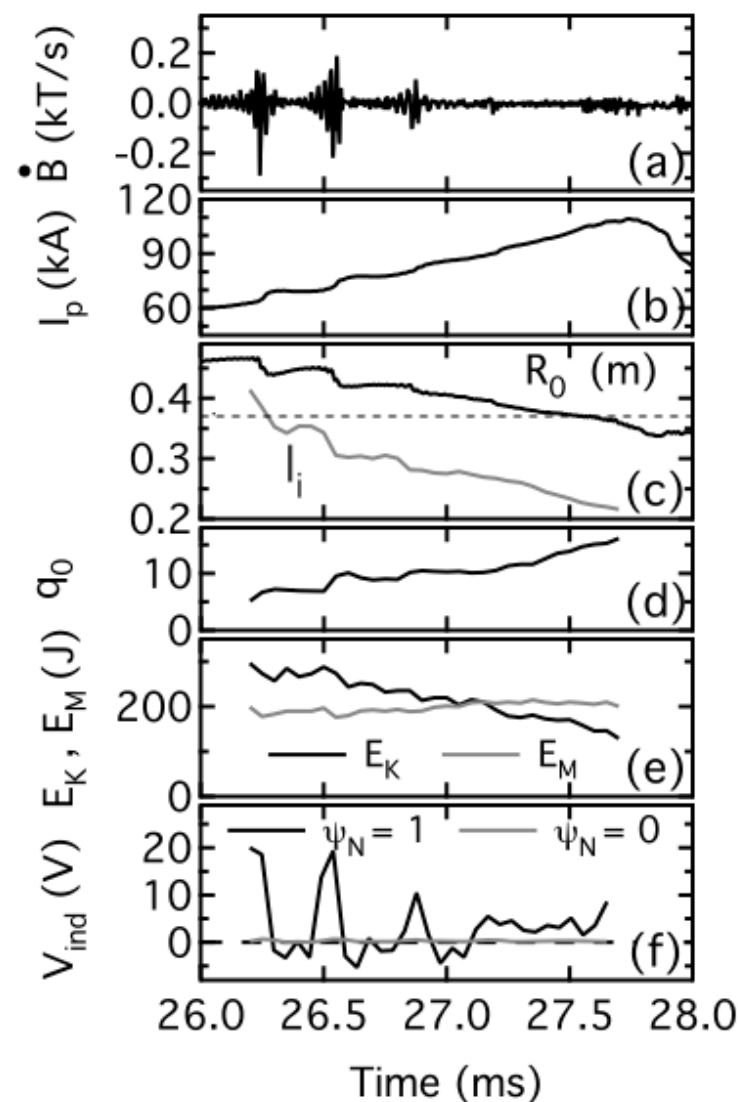
- Bursts of  $n = 1$  magnetic oscillations
  - Observed when plasma is coupled to edge current drive
  - Different in nature from inboard current injection experiments





# The magnetic topology quickly changes with each burst of MHD activity

- Each burst typically  $\sim 0.1$  ms
- With each burst...
  - $I_i$  decreases  $\rightarrow I_p$  increases
  - $R_o$  decreases  $\rightarrow$  plasma expands
  - $B_{\phi 0}$  increases  $\rightarrow q_o$  increases
  - Slight drop in  $E_k$  and  $E_m$
  - Very little change in poloidal flux at plasma edge
  - Rapid decrease in the total trapped poloidal flux



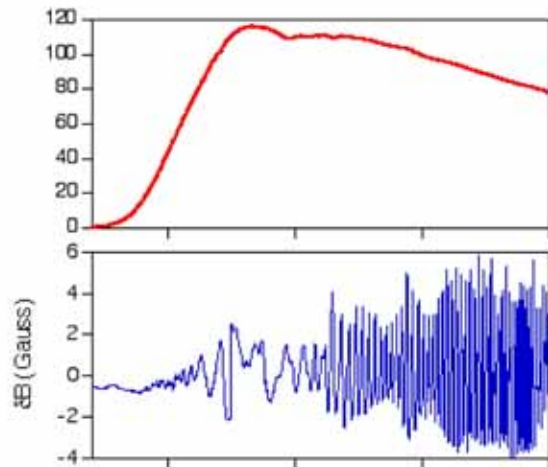
RJF ISTW 2011 • Temporally and spatially averaged  $V_{ind}$   
 $\sim 1.5$  V



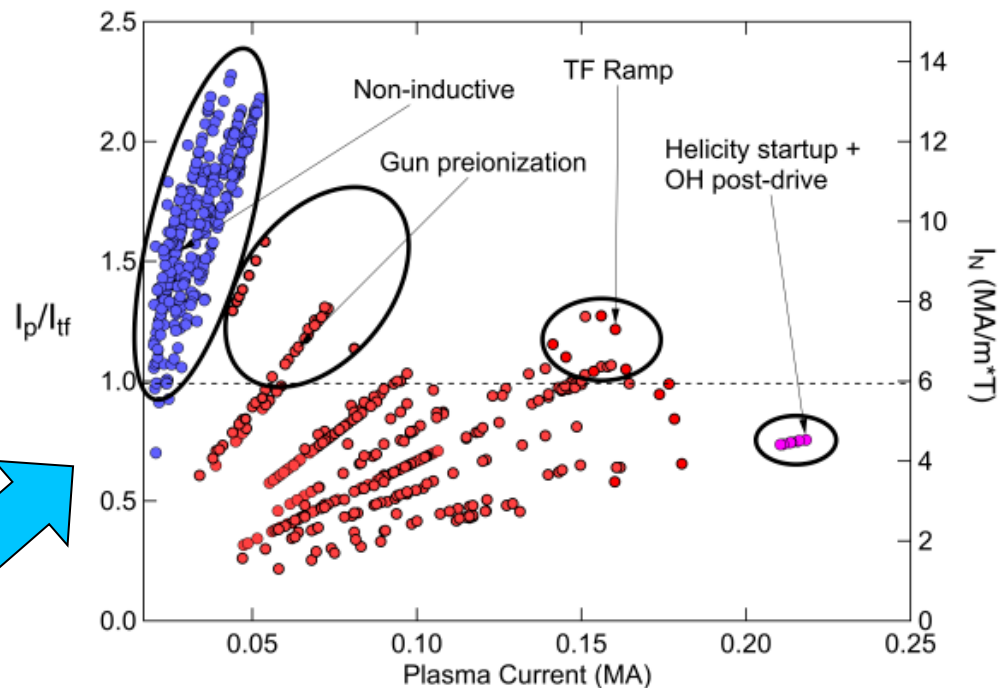
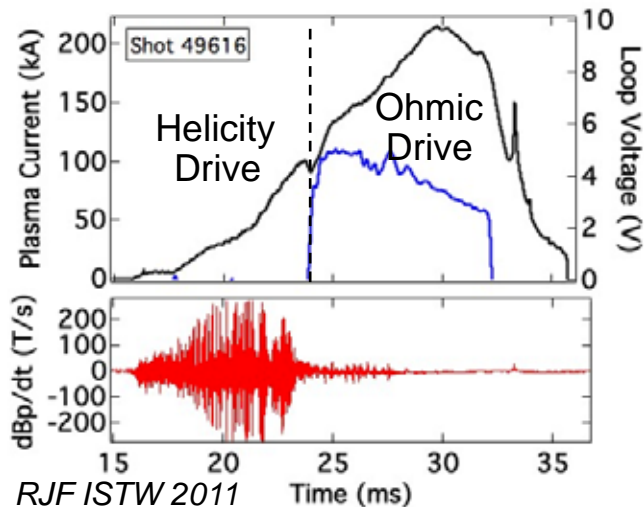


# Current Drive Tools Providing Access to High Field Utilization Regime

OH only = large 2/1 modes limit  $I_p$



HI startup = MHD quiescent

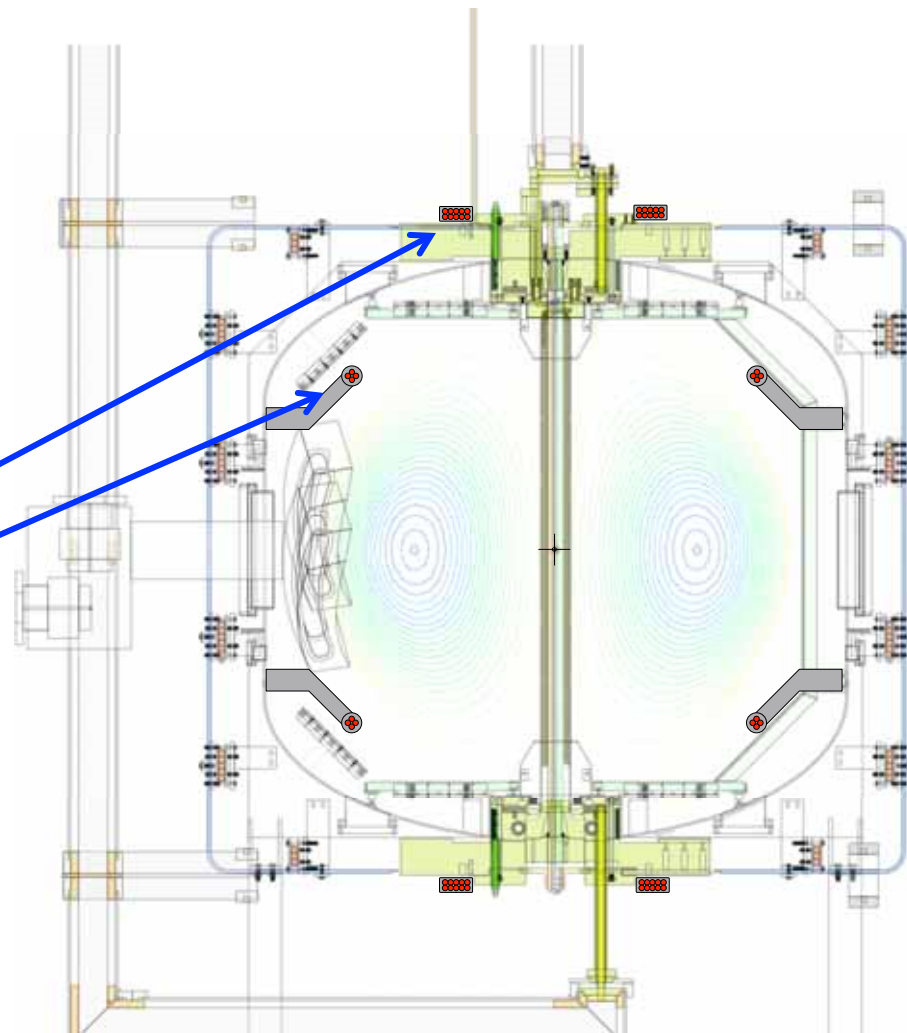


- Helicity injection startup and Ohmic sustainment provides MHD-stable profiles at  $I_p/I_{TF} < 1$
- Need to extend to higher  $I_p$ , then to low  $I_{TF}$  for high  $I_N$  and high  $\beta_T$  as  $A \approx 1$



# Medium-Term Upgrades Will Allow Further Tests of Point-Source Helicity Injection

- Gun-electrode Evolution
  - Passive electrode material variations
    - C electrode being installed
  - Separate plasma gun and electrode
- Power Supplies, Heating
  - New helicity injection power: 2 kV, 15 kA
  - Double TF current: *Taylor limit increase*
  - Commission HHFW system: *electron heating*
- Expanded PF Coil Set and control
  - Internal coils for radial position control
  - New external divertor coils
  - Implement GA Plasma Control System
- Diagnostic Additions
  - Multipoint Thomson Scattering
  - High-speed  $T_i(r,t)$ 
    - *Anomalous reconnection heating*

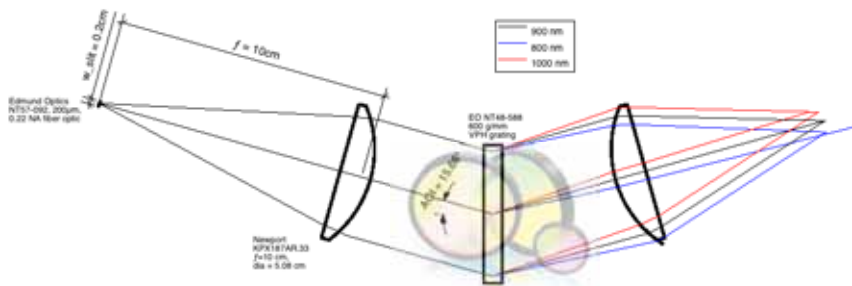




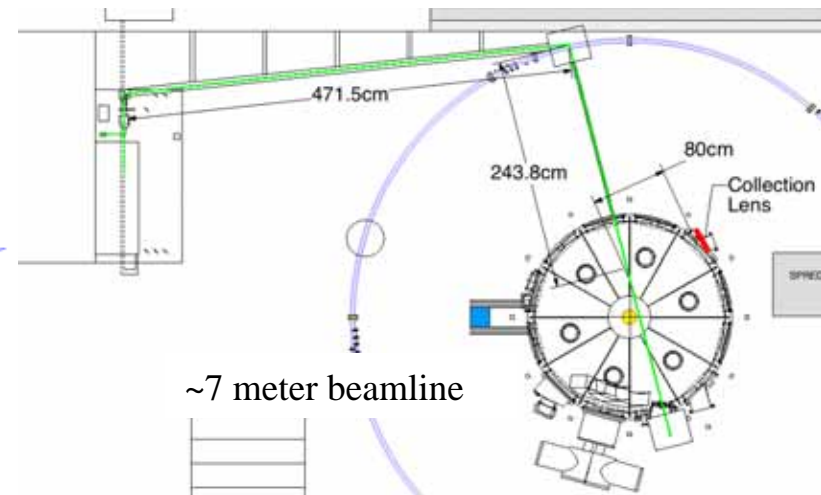
# Thomson Scattering system uses new technologies for visible wavelength system

- Frequency doubled Nd:YAG laser provides  $\sim 10^{18}$  photons
- For typical PEGASUS plasma,  $n_{\text{scattered}} \sim 10^4$  photons
- **VPH grating** efficiency  $> 85\%$  for  $\lambda_{\text{inc}} = 532 - 632$  nm
- **Gen III image intensifiers**  $\sim 50\%$  efficient in visible region
- $\sim 6$  ns ICCD gating provides easy detector technology

Laser Specifications	Value
Output Energy at 532 nm	$\geq 2000$ mJ
Beam diameter at head	12 mm
Beam diameter at waist	3 mm
Pointing stability	$\leq 50$ $\mu$ rad
Divergence	$\leq 0.5$ mrad
Repetition Rate	$\leq 10$ Hz
Pulse length	$\geq 10$ ns



Volume Phase Holographic (VPH) Grating





# HI Conclusion: High- $I_p$ Non-Solenoidal Startup via Point-Source Helicity Injection Looks Promising

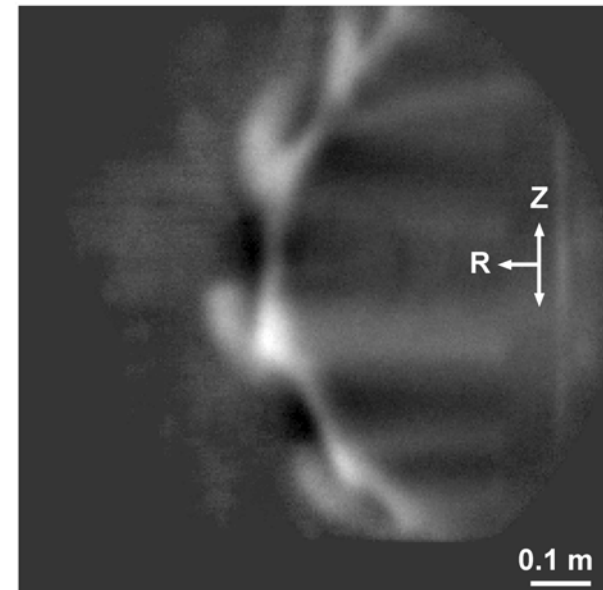
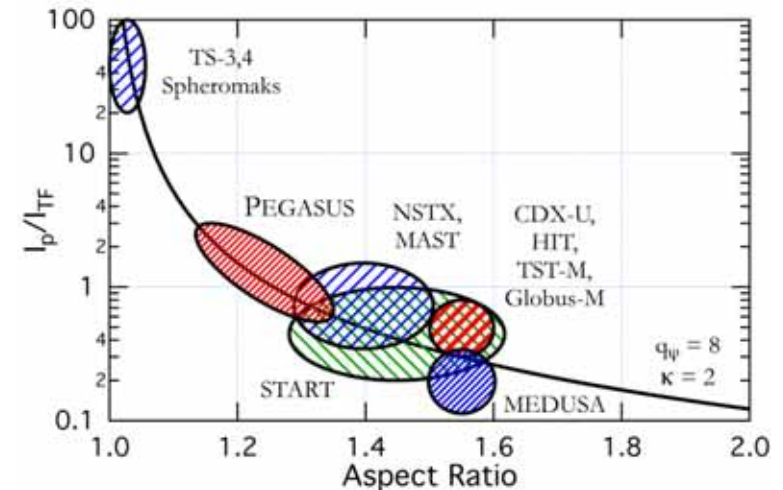
- Significant progress with non-solenoidal startup of ST
  - $I_p \sim 0.17$  MA using helicity injection and outer-PF rampup
  - Using understanding of helicity balance and relaxation current limit to guide hardware and operational changes
    - So far, predicted scalings supported
  - Goal  $\approx 0.3$ - $0.4$  MA non-solenoidal  $I_p$  to extrapolate to next level/NSTX
    - Outstanding physics questions:  $\lambda_{\text{edge}}$ ,  $Z_{\text{inj}}$ , confinement, *etc.*
  - Deploying plasma diagnostics to better understand properties
- Exploration of high  $I_N$ ,  $\beta_t$  space facilitated by  $j(r)$  tools
  - $I_p/I_{\text{TF}} > 2$ ,  $I_N > 14$  achieved; extend operation to high  $I_p$ ,  $n_e$  for high  $\beta_t$
- Holds Promise as a Scalable Non-Inductive Startup Technique
  - Simpler injection system using plasma gun – passive electrode combination may be feasible





# Some Low-A ST ITER-relevance: Access to Peeling Instability and Conditions to Measure $J$

- Spherical tokamaks naturally provide strong peeling drive
  - Toroidal field utilization  $I_p/I_{TF} \sim j_{||}/B$
- PEGASUS accesses peeling modes
  - Strong  $j_{||}/B$  MA/m<sup>2</sup>-T at
  - Comparable to DIII-D in H-mode
- Machine parameters permit internal edge measurements
  - Short pulse lengths (< 50 ms)
  - Modest  $T_e < 200$  eV

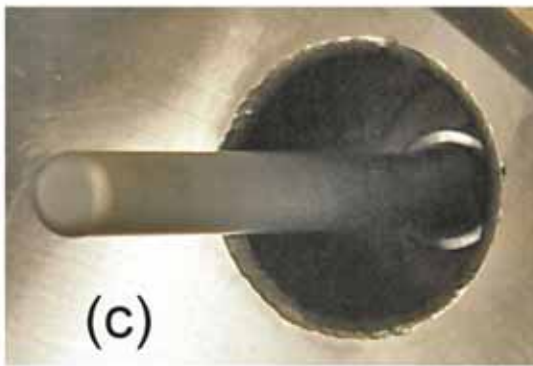
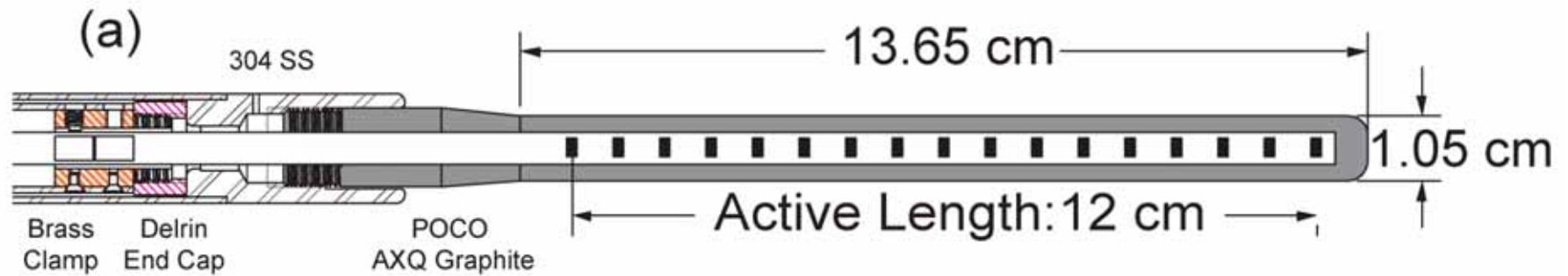


Bongard *et al.*, Phys. Rev. Lett. **107**, 035003 (2011)





# PEGASUS Hall Probe Deployed to Measure J



- Solid-state InSb Hall sensors
  - Sypris model SH-410
- Slim C armor as low-Z PFC
  - Minimizes plasma perturbation
- 16 channels, 7.5 mm radial resolution
- 25 kHz bandwidth



## $J_\phi(R,t)$ Calculable Directly from Ampère's Law

$$\mu_0 J_\phi = (\nabla \times \mathbf{B})_\phi = \frac{\partial B_R}{\partial Z} - \frac{\partial B_Z}{\partial R}$$

- Simplest test follows from  $B_R(Z)$  or  $B_Z(R)$  measurements
- Petty\* solves for an off-midplane  $B_Z(R)$  measurement set and an elliptical plasma cross-section:

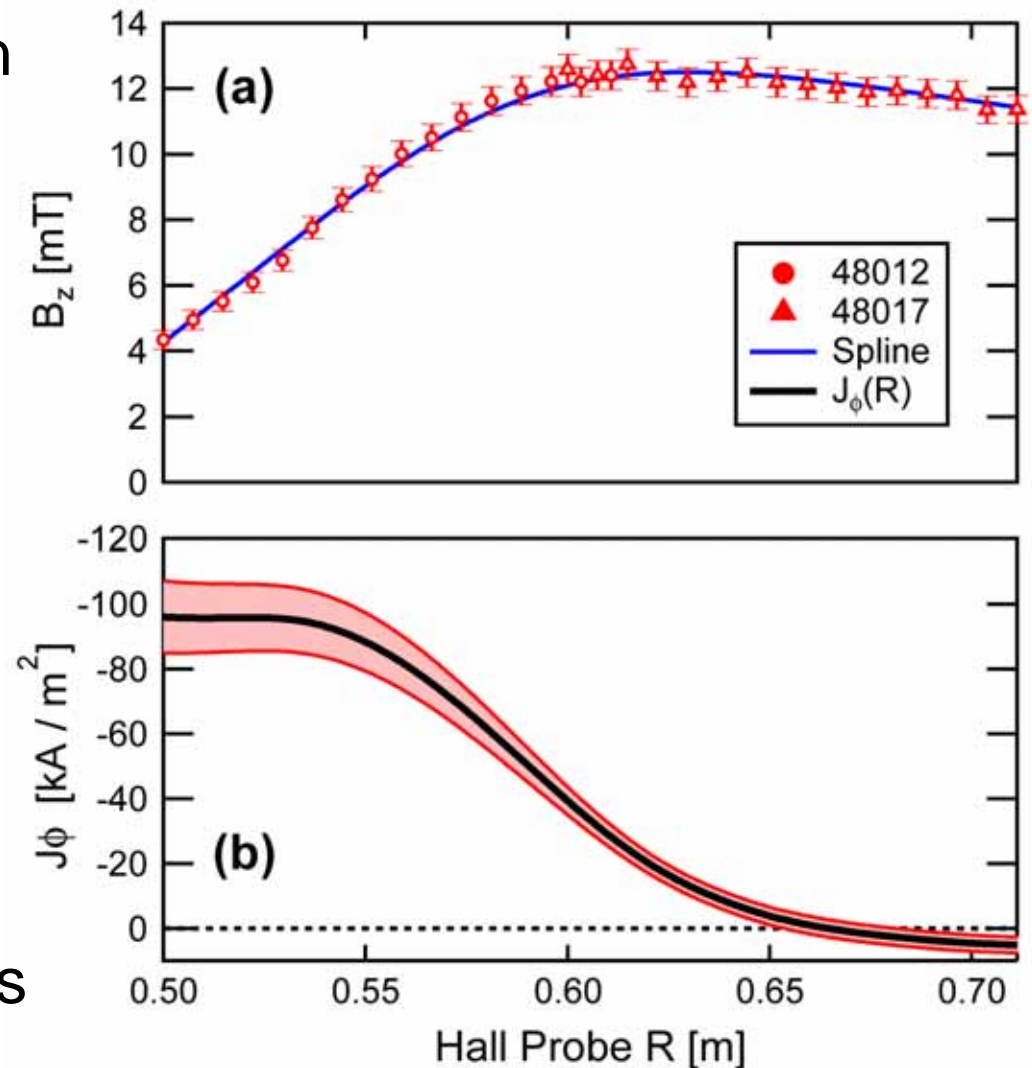
$$\mu_0 J_\phi = -\frac{B_Z}{\kappa^2 (R - R_0)} \left( 1 - \frac{Z^2 R_0}{\kappa^2 R (R - R_0)^2} \right) - \frac{dB_Z}{dR} \left( 1 + \frac{Z^2}{\kappa^4 (R - R_0)^2} \right)$$

- Does not make assumptions on shape of  $J(R)$



# Direct $J_\phi(R)$ Profiles Obtained in PEGASUS

- Straightforward J estimation
  - Obtain Hall Probe  $B_z(R,t)$
  - Compute  $dB_z/dR$  using interpolated smoothing spline\*
  - Compute  $J_\phi(R,t)$  given geometry
- Resultant  $J_\phi(R,t)$  consistent with  $I_p$ , MHD evolution
- Radial span extendible with multi-shot averaging
- Higher-order shaping effects negligible within errors

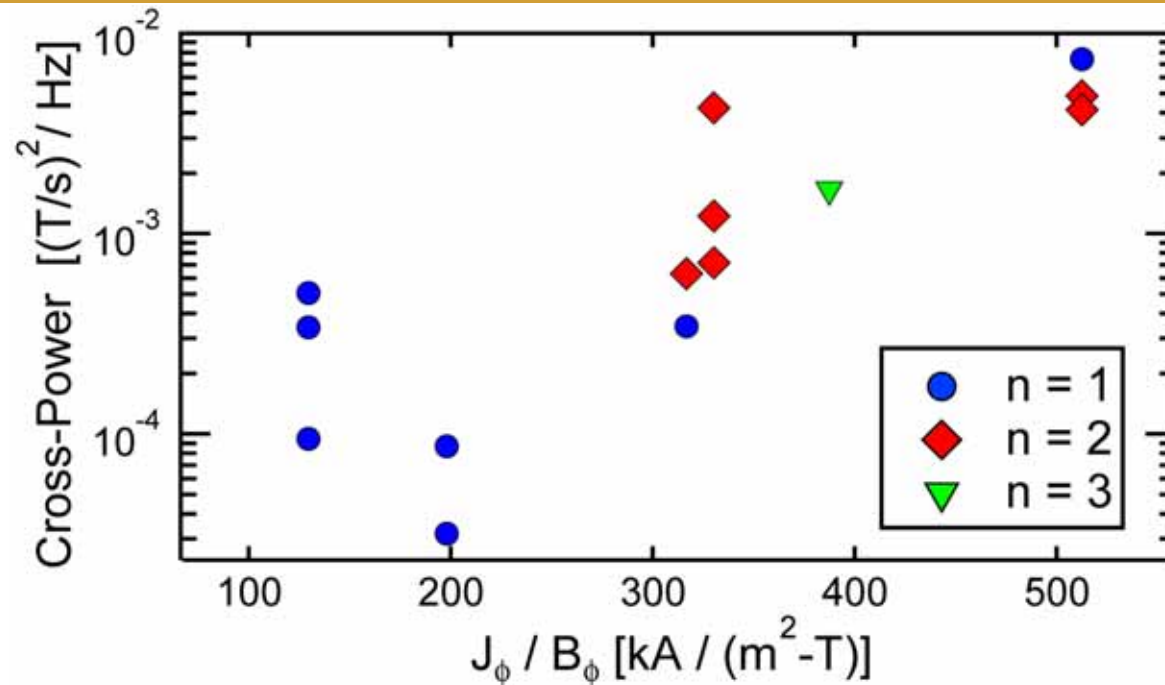


Bongard *et al.*, Phys. Rev. Lett. **107**, 035003 (2011)





# Peeling MHD Strongly Scales with Theoretical Drive

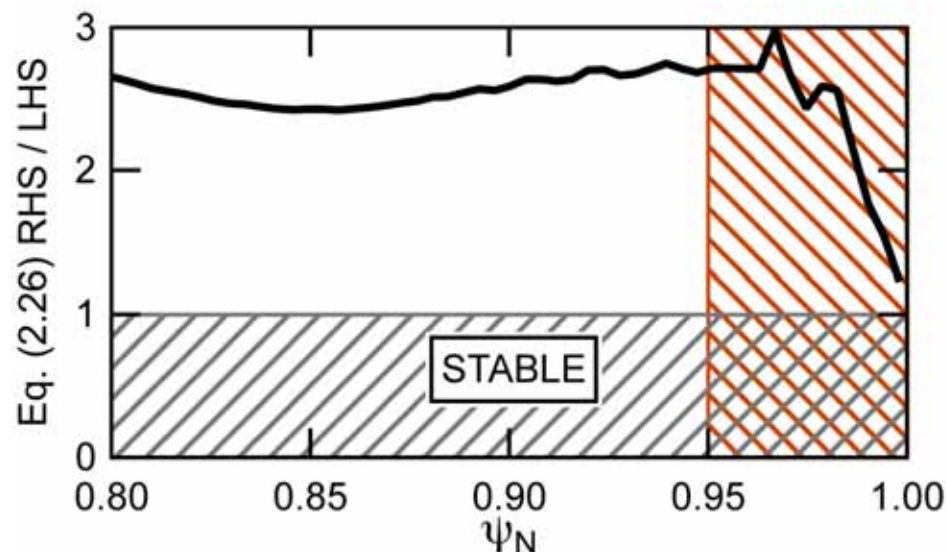


- Mode helicities estimated from port 8 Mirnov array
  - $n < 3$  via cross-phase analysis
  - $m_{\text{lab}} \geq 10$  via radial decay rate
  - $10 \leq m_{\text{lab}} / n \leq 30$  ( $\psi \downarrow N > 0.9$ )
- MHD power spans two orders of magnitude with factor-of-five variation in J/B

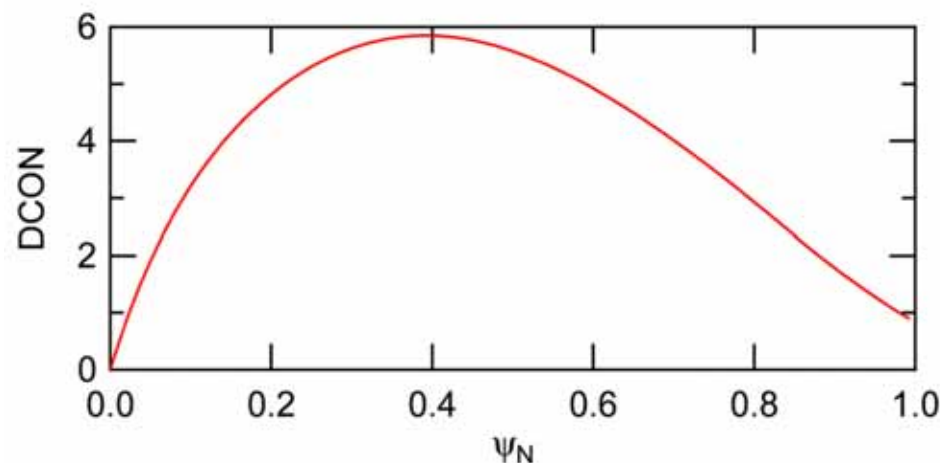


# Stability Analysis Confirms Peeling Instability

- Analytic peeling criterion computed from Hall-constrained equilibrium indicates instability
  - More than factor of two in region of optimal  $\langle J \downarrow \phi \rangle$  constraint
- Free-boundary ideal stability analysis performed with DCON
  - Indicates instability to  $m/n = 19/1$  external kink
- Both methods agree with experiment



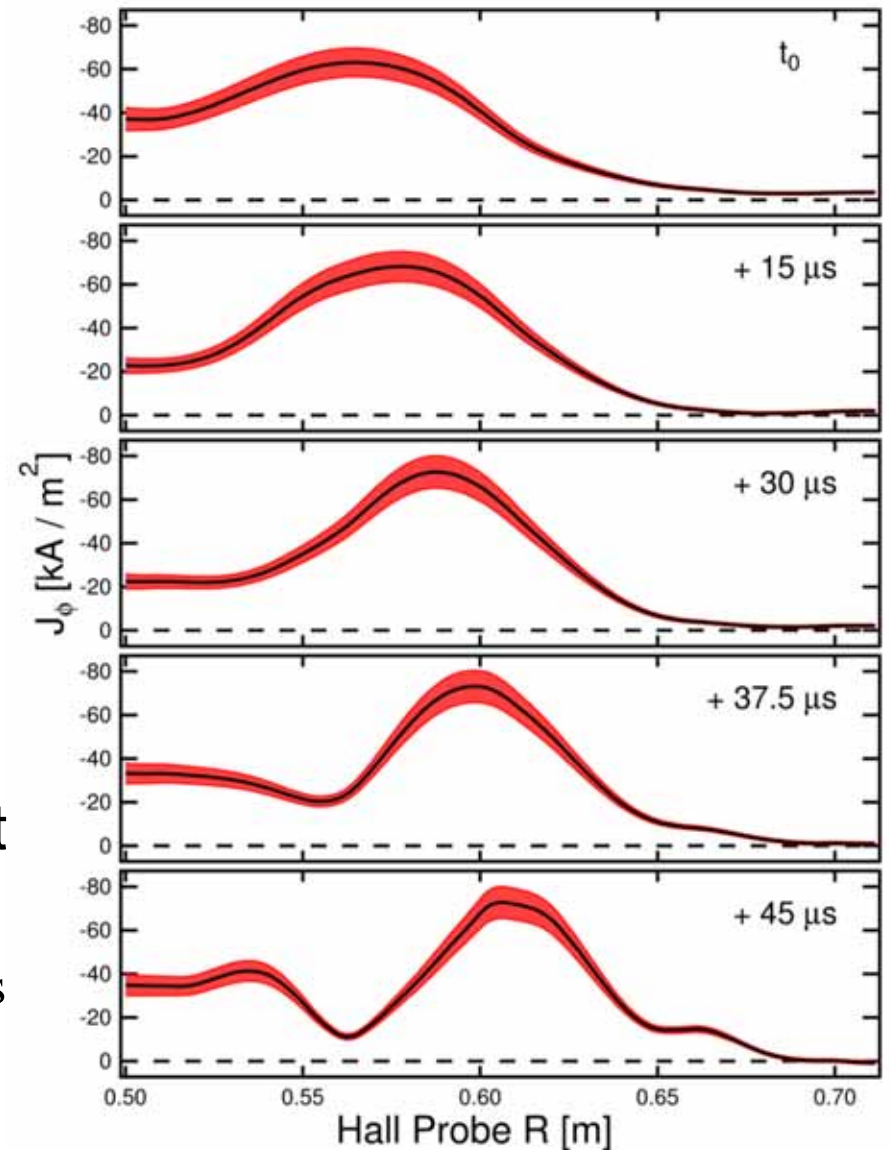
Bongard *et al.*, Phys. Rev. Lett. **107**, 035003 (2011)





# $J_{\text{edge}}$ Dynamics Measured on ELM Timescales

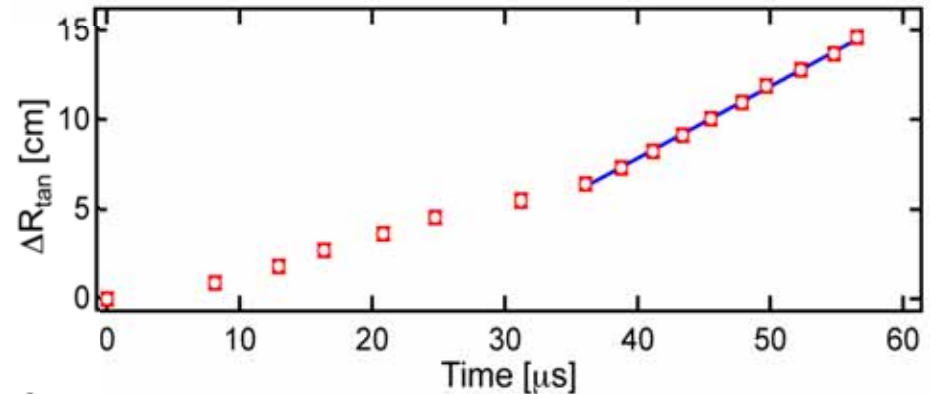
- $J_{\text{edge}}$  resolved during peeling filament generation
- Propagating filament forms from initial “current-hole”  $J_{\text{edge}}$  perturbation
  - Validates formation mechanism hypothesized by EM blob transport theory
- Filament carries toroidal current  $I_f \sim 100\text{--}220\text{ A}$ 
  - Comparable to MAST ELM estimates
  - $I_f < 0.2\%$  of  $I_p$



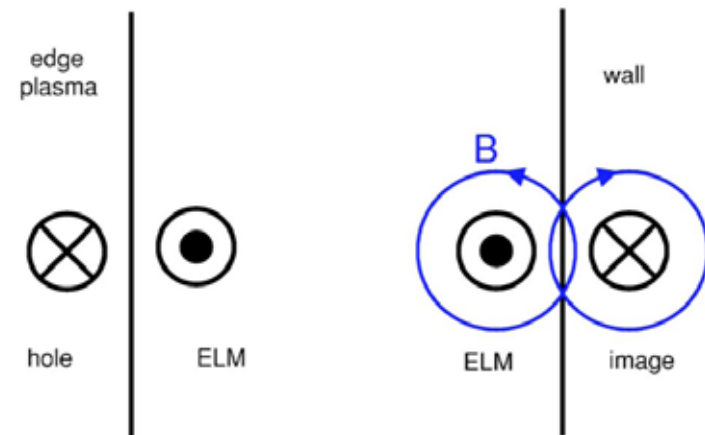
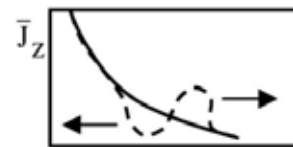


# Filament Radial Motion Qualitatively Consistent with Electromagnetic Blob Transport

- Trajectory of detached filament tracked with 275 kHz imaging
  - Radially accelerates, followed by constant velocity motion
- Magnetostatic repulsion\* plausibly contributes to dynamics
  - Current-hole  $\mathbf{J} \times \mathbf{B}$  drives  $aR$
  - Transition at  $\sim 35 \mu\text{s}$  comparable to healing time of current-hole
- Measured  $VR$  comparable to available EM blob models\*\*
  - $VR \sim 4 \text{ km/s}$ ;  $VR, IB \sim 8 \text{ km/s}$
  - Agrees to  $O(1)$  accuracy of theory



Bongard *et al.*, Phys. Rev. Lett. **107**, 035003 (2011)



\*: Myra, Phys. Plasmas **14**, 102314 (2007)

\*\* : Myra *et al.*, Phys. Plasmas **12**, 092511 (2005)





# Peeling Mode / ELM Conclusions

- Direct measurements of  $J_{\text{edge}}$  conducted with Hall probe
  - Direct analysis, equilibrium reconstruction
  - $J_{\text{edge}}$  controllable with  $dI_p/dt$
- Characteristics of Peeling Modes Consistent with Theory
  - Macroscopic features: Low-n, high-m external kink
  - Onset consistent with ideal MHD, analytic peeling stability theories
  - Observed MHD scales with measured J/B peeling drive
  - Coherent, propagating filaments
- $J_{\text{edge}}$  dynamics supports current-hole & EM blob hypotheses
  - Nonlinear filaments generated from current-hole  $J_{\text{edge}}$  perturbation
  - Transient magnetostatic repulsion
  - Constant- $V_R$  propagation in agreement with available EM blob theory



# HI Conclusion: High- $I_p$ Non-Solenoidal Startup via Point-Source Helicity Injection Looks Promising

- Significant progress with non-solenoidal startup of ST
  - $I_p \sim 0.17$  MA using helicity injection and outer-PF rampup
  - Using understanding of helicity balance and relaxation current limit to guide hardware and operational changes
    - So far, predicted scalings supported
  - Goal  $\approx 0.3$ - $0.4$  MA non-solenoidal  $I_p$  to extrapolate to next level/NSTX
    - Outstanding physics questions:  $\lambda_{\text{edge}}$ ,  $Z_{\text{inj}}$ , confinement, *etc.*
  - Deploying plasma diagnostics to better understand properties
- Exploration of high  $I_N$ ,  $\beta_t$  space facilitated by  $j(r)$  tools
  - $I_p/I_{\text{TF}} > 2$ ,  $I_N > 14$  achieved; extend operation to high  $I_p$ ,  $n_e$  for high  $\beta_t$
- Holds Promise as a Scalable Non-Inductive Startup Technique
  - Simpler injection system using plasma gun – passive electrode combination may be feasible